AFFDL-TR-78-26

LEVEL II

ⓔ

②

DESIGN AND TEST OF AN ANNULAR STING SUPPORT CONCEPT FOR AFTBODY NOZZLE WIND TUNNEL TESTING

Aerodynamics and Airframe Branch
Aeromechanics Division

April 1978

D D C
RECEIVED
AUG 3 1978
E

TECHNICAL REPORT AFFDL-TR-78-26

Final Report for Period January 1976 - September 1977

AIR FORCE FLIGHT DYNAMICS LABORATORY
AIR FORCE WRIGHT AERONAUTICAL LABORATORIES
AIR FORCE SYSTEMS COMMAND
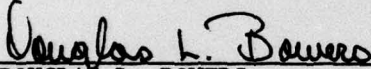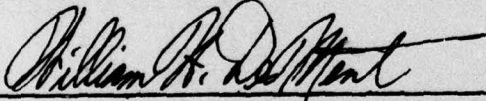WRIGHT-PATTERSON AIR FORCE BASE, OHIO 45433

78 07 31 057

NOTICE

When Government drawings, specifications, or other data are used for any purpose other than in connection with a definitely related Government procurement operation, the United States Government thereby incurs no responsibility nor any obligation whatsoever; and the fact that the government may have formulated, furnished, or in any way supplied the said drawings, specifications, or other data, is not to be regarded by implication or otherwise as in any manner licensing the holder or any other person or corporation, or conveying any rights or permission to manufacture, use, or sell any patented invention that may in any way be related thereto.

This report has been reviewed by the Information Office (OI) and is releasable to the National Technical Information Service (NTIS). At NTIS, it will be available to the general public, including foreign nations.

This technical report has been reviewed and is approved for publication.

DOUGLAS L. BOWERS
Project Engineer

FOR THE COMMANDER

WILLIAM H. DeMENT, Acting Chief,
Aerodynamics & Airframe Branch
Aeromechanics Division

SECURITY CLASSIFICATION OF THIS PAGE *(When Data Entered)*

REPORT DOCUMENTATION PAGE		READ INSTRUCTIONS BEFORE COMPLETING FORM
1. REPORT NUMBER AFFDL-TR-78-26	2. GOVT ACCESSION NO.	3. RECIPIENT'S CATALOG NUMBER
4. TITLE *(and Subtitle)* DESIGN AND TEST OF AN ANNULAR STING SUPPORT CONCEPT FOR AFTBODY NOZZLE WIND TUNNEL TESTING.		5. TYPE OF REPORT & PERIOD COVERED Final Report. 1 January 1976-1 September 1977
		6. PERFORMING ORG. REPORT NUMBER
7. AUTHOR(s) Douglas L. Bowers		8. CONTRACT OR GRANT NUMBER(s)
9. PERFORMING ORGANIZATION NAME AND ADDRESS Aerodynamics and Airframe Branch (FXM) Air Force Flight Dynamics Laboratory Wright-Patterson Air Force Base, OH 45433		10. PROGRAM ELEMENT, PROJECT, TASK AREA & WORK UNIT NUMBERS Project 2404 Task 240410 Job Order No. 24041009
11. CONTROLLING OFFICE NAME AND ADDRESS Air Force Flight Dynamics Laboratory Wright-Patterson Air Force Base, OH 45433		12. REPORT DATE April 1978
		13. NUMBER OF PAGES 63
14. MONITORING AGENCY NAME & ADDRESS*(if different from Controlling Office)* 2404		15. SECURITY CLASS. *(of this report)* Unclassified
		15a. DECLASSIFICATION/DOWNGRADING SCHEDULE

16. DISTRIBUTION STATEMENT *(of this Report)*

Approved for public release; distribution unlimited

17. DISTRIBUTION STATEMENT *(of the abstract entered in Block 20, if different from Report)*

18. SUPPLEMENTARY NOTES

19. KEY WORDS *(Continue on reverse side if necessary and identify by block number)*

Exhaust Nozzles	Turbojet Engines
Wind Tunnels	Turbofan Engines
Nozzle Flow	Testing Techniques
Transonic Flow	

20. ABSTRACT *(Continue on reverse side if necessary and identify by block number)*

The annular sting support concept for aftbody nozzle testing supports the model through the exhaust nozzles, provides high pressure air to simulate the exhaust plume to enter the model, and provides a path for instrumentation lines to be routed out of the model. The support concept, experimental model, and supporting analytical studies are described. Experimental data for the aftbody nozzle contours are compared for a free jet test and the annular sting support test. Also the results of an analytical prediction of the nozzle boattail pressure

DD 1 JAN 73 1473   EDITION OF 1 NOV 65 IS OBSOLETE

SECURITY CLASSIFICATION OF THIS PAGE *(When Data Entered)*

78 07 31 057

20. Abstract (Continued)

distribution and wind tunnel wall effects are described. Test results and experimental data comparisons indicate that the annular sting support concept offers an alternate testing technique for aftbody nozzles.

FOREWORD

This report was prepared by Douglas L. Bowers of the Internal
Aerodynamics Group, Aerodynamics and Airframe Branch, Aeromechanics
Division of the Air Force Flight Dynamics Laboratory (AFFDL/FXM),
Wright-Patterson Air Force Base, Ohio. This research was conducted
under Work Unit Number 24041009, "Design and Analysis of Advanced
Strategic and Tactical Military Aircraft Exhaust Nozzle Systems".
A portion of this effort is summarized in AIAA Paper No. 77-961,
"Investigation of the Annular Sting Support Concept for Aftbody Nozzle
Testing" presented at the AIAA/SAE 13th Propulsion Conference, July 1977.
This research was conducted from 1 January 1976 - 1 September 1977.

ACCESSION for

NTIS	White Section	X
DDC	Buff Section	☐
UNANNOUNCED		☐
JUSTIFICATION		

BY

DISTRIBUTION/AVAILABILITY CODES

Dist.	AVAIL. and/or SPECIAL
A	

TABLE OF CONTENTS

LIST OF FIGURES

LIST OF FIGURES (CONTINUED)

LIST OF TABLES

LIST OF SYMBOLS

A   - geometric area

C_p - pressure coefficient $\left(\dfrac{\text{local pressure - freestream pressure}}{\text{freestream dynamic pressure}} \right)$

ID   - inner diameter, inches

L   - length of nozzle boattail

M   - Mach number

NPR   - nozzle pressure ratio $\left(\dfrac{\text{nozzle throat total pressure}}{\text{freestream static pressure}} \right)$

OD   - outer diameter, inches

R   - geometric radius

WT   - wall thickness, inches

X   - distance along nozzle boattail from nozzle exit

θ - angular measure, degrees

Subscripts

max - maximum

n   - internal nozzle

proj - projected

SECTION I

INTRODUCTION

Advanced aircraft airframe systems and advanced propulsion systems have imposed severe accuracy requirements on experimental data acquisition and analysis. As the afterbody nozzle configurations evolve, the absolute performance increments between separate configurations decrease. These absolute performance increments must be corrected, however, for model support effects for conventional aircraft aftbody nozzle testing techniques. The testing required to obtain these corrections uses expensive resources which could be utilized to increase the experimental data directly applicable to the investigation. Testing alternate support systems in combination, such as strut/sting or strut/wingtip is the state-of-the-art method to produce the support interference corrections. An alternate model support technique for nozzle aftbody testing which may eliminate the support interference corrections is the annular sting support concept. The annular sting concept supports the model by a sting through the exhaust nozzle, provides a path for high pressure air to enter the model and reverses the flow to simulate the exhaust plume and a path for instrumentation lines to be routed from the model. While this concept has been previously investigated, those efforts were for full aircraft models over a limited range of test conditions and the experimental results are not easily analyzed to determine the data variance due to the annular sting. This document describes design, test conditions, and results of an experimental effort to determine the feasibility of the annular sting concept for aftbody nozzle testing. The test model utilized was heavily instrumented with external static pressure orifices in the boattail region in order to evaluate the annular sting versus a free jet testing technique. The proper simulation of jet effects, critical in aftbody nozzle testing, is addressed for both the free jet and the annular sting. Schlieren photographs and analytical procedures were used to assess the differences in exhaust plume structure and the impact on the aftbody flow field. An analytical portion of this effort predicted the nozzle aftbody pressure coefficient distributions by various methods.

This document describes the design concept and mechanical features
of the annular sting. A summary of the test results including external
pressure coefficient distributions and exhaust plume contours for the
free jet and the annular sting is provided. Also discussed are the
analytical predictions and considerations of the applicability of the
annular sting concept for aftbody nozzle wind tunnel testing.

SECTION II

DISCUSSION

1. CONCEPT DESIGN PHILOSOPHY

Critical to the applicability of the annular sting support concept to nozzle testing is the ability of the testing technique to provide jet effects of a flowing exhaust plume and still retain the capability to safely support the experimental model. The annular sting concept must, therefore, support the model safely within the wind tunnel environment, duct high pressure air into and out of the model with sufficient mass flow and pressure to simulate a free jet exhaust plume, and provide a conduit for a minimum number of instrumentation lines going out of the model. In the extremes of sting diameter, the annular sting would have either an infinitely small sting diameter and be a free jet with no capability to support the model or it would have a sting diameter near the nozzle exit diameter and be a solid plume without the flow entrainment and wake effects attributed to a flowing jet. If the annular sting concept is to be acceptable for a nozzle aftbody testing technique an optimum sting diameter must exist between these two extremes. For this effort a support sting of constant diameter was used for all nozzles tested. The varying throat areas for the nozzles provided different relationships of nozzle flow area at nozzle throat and solid body interference at the nozzle exit. The test results indicate that the sting diameter with respect to the nozzle throat diameter may be too large to provide adequate jet effects.

Care must be taken when designing the internal nozzle flow parameters. The free jet nozzle to be tested with an annular sting has a specific internal area ratio (convergent-divergent nozzle), that is, the ratio of the throat flow area to the exit flow area and internal nozzle wall divergence angle. To provide the same initial plume angle at identical nozzle pressure ratios, the free jet and annular sting exhaust nozzle must have these internal flow parameters equivalent. The presence of the sting, however, affects the flow area ratio and subsequently the

internal nozzle divergence angle. The internal nozzle contour of the free jet exhaust nozzle must be modified by changes in nozzle throat diameter and nozzle internal length, throat station to exit station, to accommodate the support sting and maintain the internal geometric relationships. Specific internal flow parameter values are presented in a subsequent portion of this text.

The conceptual design for the annular sting utilized in this experimental program is shown in Figure 1. The coannular sting supports the cone cylinder model internally at forward and aft attach points. Geometric details of the stainless steel support sting are displayed. The high pressure air for the exhaust plume simulation is ducted through the outer support sting (around the inner instrumentation sting) to the front of the model where the high pressure air is turned to flow aft to the nozzle exit. The inner instrumentation sting is a duct for scanivalve electrical power and output lines and a minimum number of pressure lines. Incorporation of an internal scanivalve to sense the external boattail pressures reduced the requirement for a large number of pressure lines to be routed from the body and facilitated model design. The nozzles utilized in this test were manufactured with no splits to eliminate flow-field interference. This required the model changes to be performed in the following sequence: 1) model nose removed, 2) pressure and electrical lines in inner sting disconnected, and 3) entire assembly pulled forward and off the support sting. For this relatively small model, this proved to be a mechanically feasible procedure to conduct model changes in a small wind tunnel. A photograph of the wind tunnel installation is shown in Figure 2. Large models may require split nozzles to facilitate changes.

The nozzle contours chosen for this investigation were tested in a free jet apparatus as part of the General Dynamics Lightweight Fighter Program. The nozzles tested represented two engine power conditions, dry and afterburning, and a reference configuration. All nozzles were instrumented with external static pressure orifices in the nozzle boattail region. The 45 pressure ports were divided into two rows of 20 orifices each at the 180 and 315 degree circumferential locations and one row

OD = .375
ID = .305
WT = .035

INNER
INSTRUMENTATION
STING

OUTER
SUPPORT
STING

OD = 1.4
ID = 1.25
WT = .075

NOZZLE
DISCONNECT
POINT

NOZZLE TOTAL
PRESSURE PROBE

AFT
MODEL
SUPPORT

FORWARD
MODEL
SUPPORT

FLOW
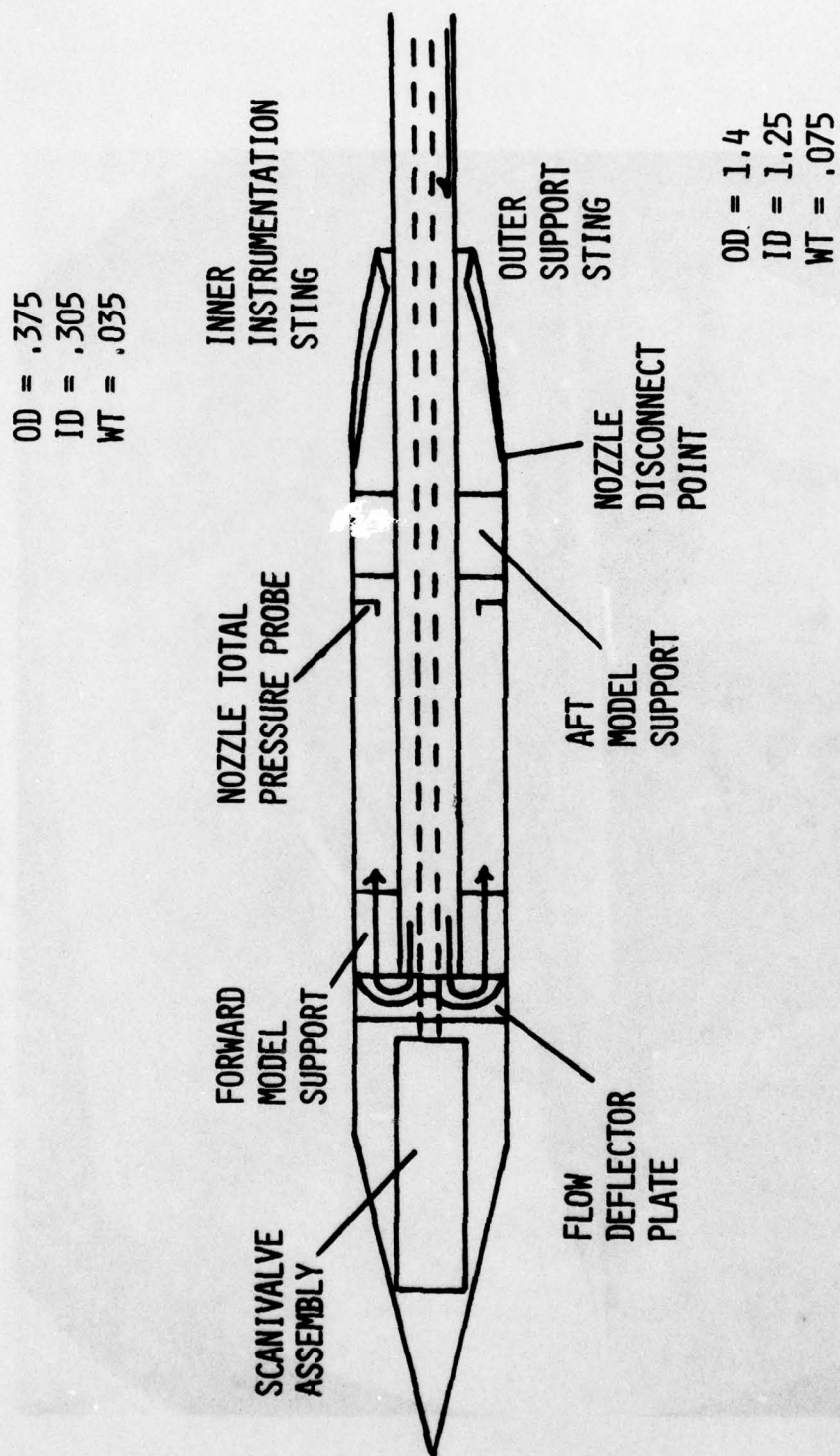DEFLECTOR
PLATE

SCANIVALVE
ASSEMBLY
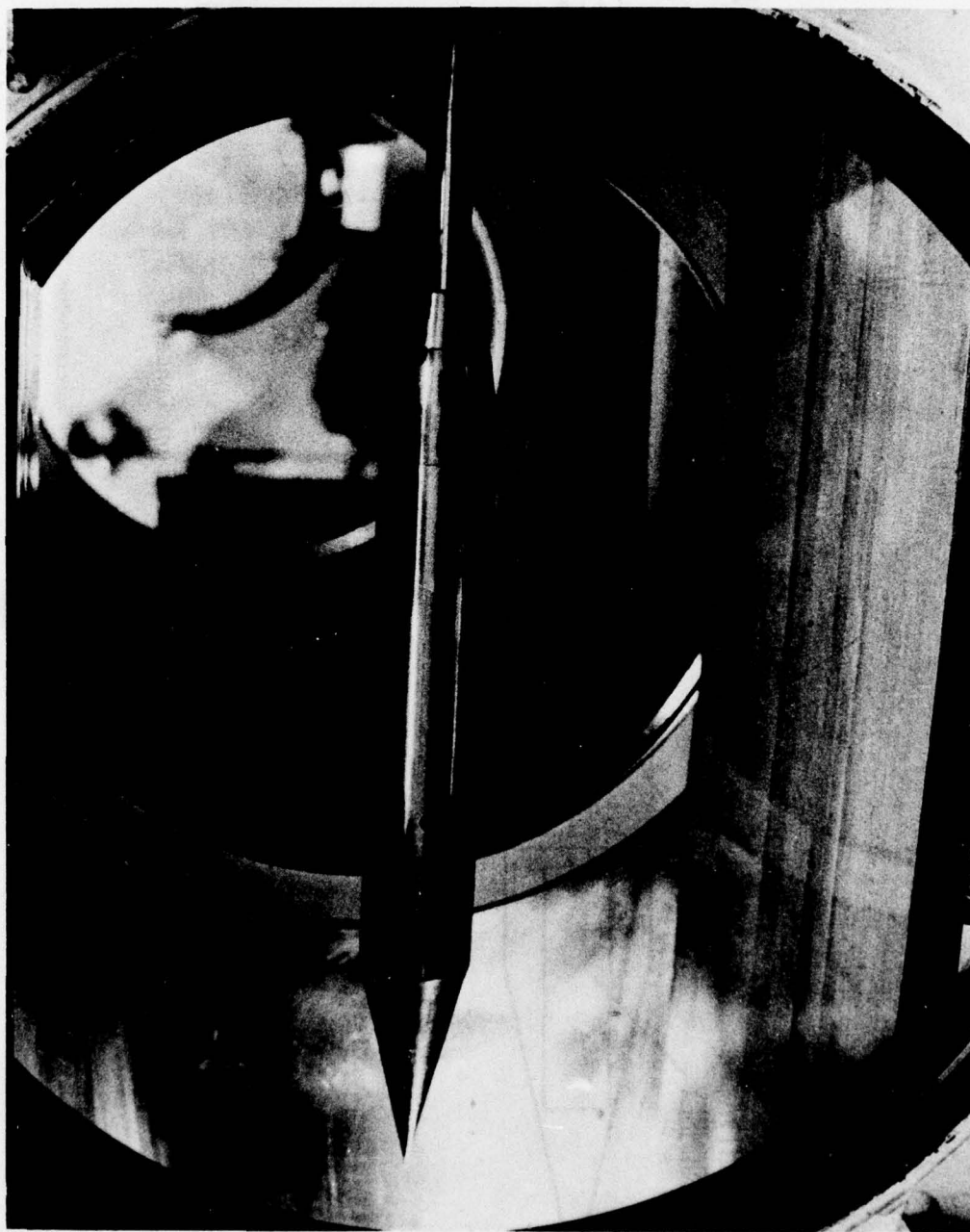
Figure 1. Annular Sting Support Concept

Figure 2. Annular Sting Support Tunnel Installation

of 5 static pressure orifices at the 45 degree location (0 degree top dead center with positive clockwise looking forward). An attempt was made to locate the static pressure orifices in similar locations on the annular sting model as the free jet model. The location of the static pressure orifices for the three nozzles is presented in Table 1.

The force and moment nozzle is representative of a reference configuration tested to satisfy inputs to thrust-drag accounting procedures. The outer support sting was fitted with a sleeve which became a portion of the nozzle inner contour. This sleeve extended two nozzle diameters downstream of the nozzle exit. A schematic of the nozzle and sting support is shown in Figure 3 and a photograph in Figure 4. The sting cross-sectional area including the sleeve was 0.487 of the nozzle throat cross-sectional area. The internal contours, including the sting, were identical for the free jet nozzle and the annular sting nozzle.

The reheat nozzle, simulating a partial afterburning power condition, was tested with modified internal contours in order to accept the annular sting support. The internal area ratio (nozzle exit flow area to nozzle throat flow area) was equivalent between the free jet nozzle and the annular sting nozzle. The internal divergence angle was not maintained due to manufacturing limitations. Corrections were made to the nozzle pressure ratio during the testing period to match the initial plume angle for both tests. This procedure is described in a later section. The internal area ratio was 1.2 for both annular sting and free jet nozzles while the internal divergence angle was 2.5° for the annular sting nozzle and 4.7° for the free jet reheat nozzle. The sting cross-sectional area was 0.446 of the nozzle throat cross-sectional area. The reheat nozzle is shown in schematic in Figure 5 and in a photograph in Figure 6.

The cruise nozzle which simulates a dry power engine condition provided the greatest design problem for the annular sting support. The internal divergence angle was maintained at 1.5° for both the annular sting nozzle and the free jet nozzle. The internal nozzle flow area was also maintained at 1.1. Ninety three percent of the nozzle throat

TABLE 1

EXTERNAL STATIC PRESSURE TAP LOCATION

Tap Number			X/L		
Row 315°	180°	45°	Force Moment	Cruise	Reheat
1	21		.968	.966	.966
2	22		.855	.846	.848
3	23		.799	.786	.789
4	24		.743	.727	.729
5	25		.687	.667	.670
6	26		.631	.607	.611
7	27		.575	.547	.552
8	28		.523	.492	.497
9	29	41	.471	.462	.470
10	30	42	.435	.424	.427
11	31	43	.407	.395	.399
12	32	44	.380	.367	.371
13	33	45	.350	.336	.336
14	34		.326	.312	.311
15	35		.309	.283	.26
16	36		.266	.254	.232
17	37		.214	.198	.204
18	38		.161	.139	.141
19	39		.109	.083	.085
20	40		.056	.013	.015

X/L
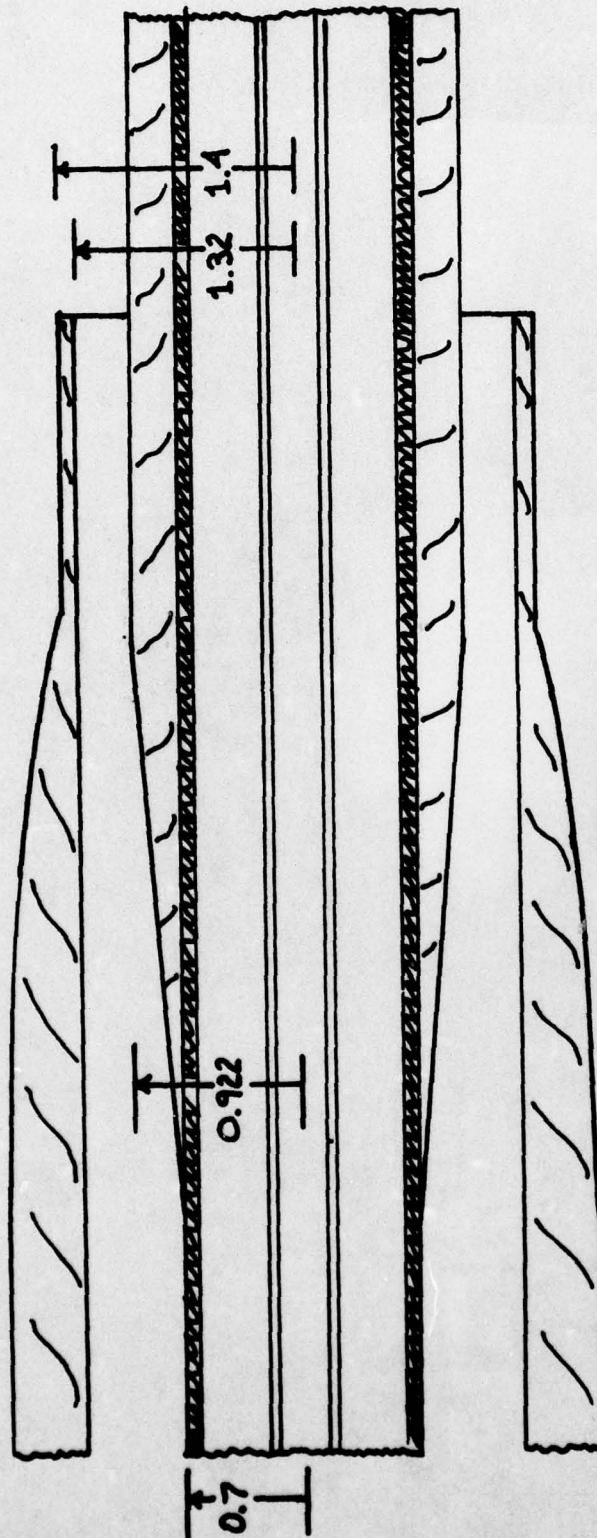
Nozzle Boattail

L

8
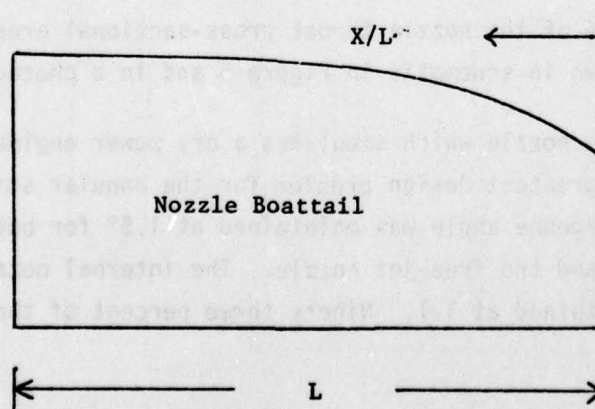
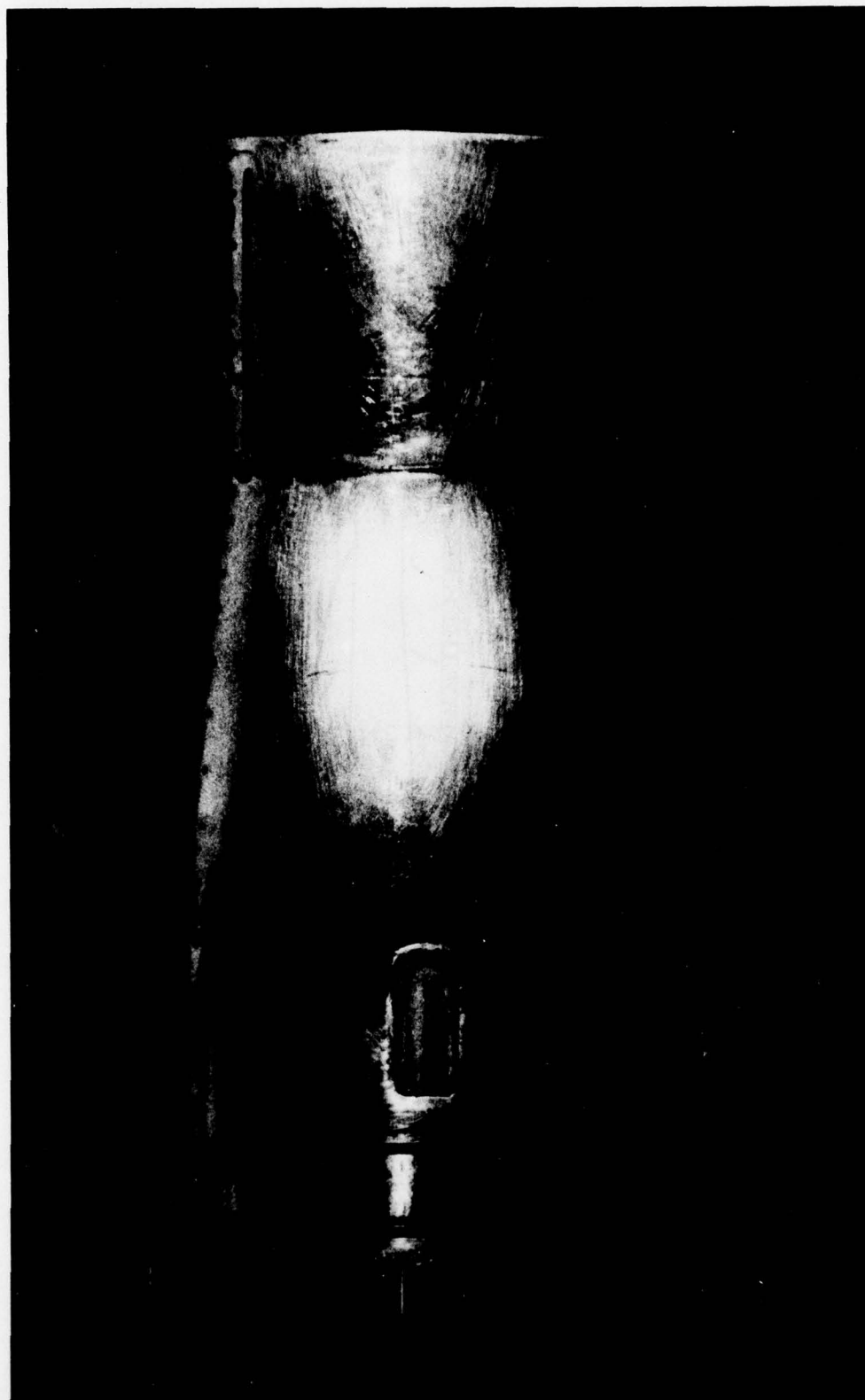Figure 3. Force and Moment Nozzle Schematic
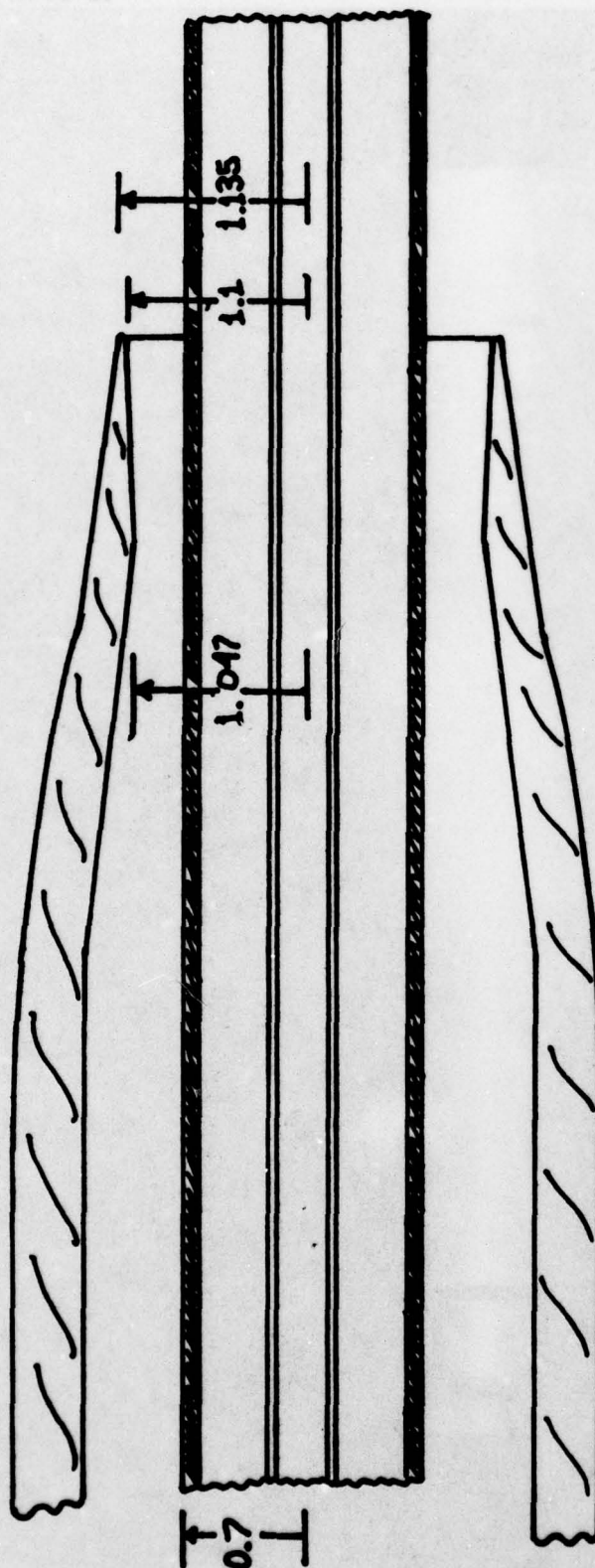
Figure 4. Force and Moment Nozzle
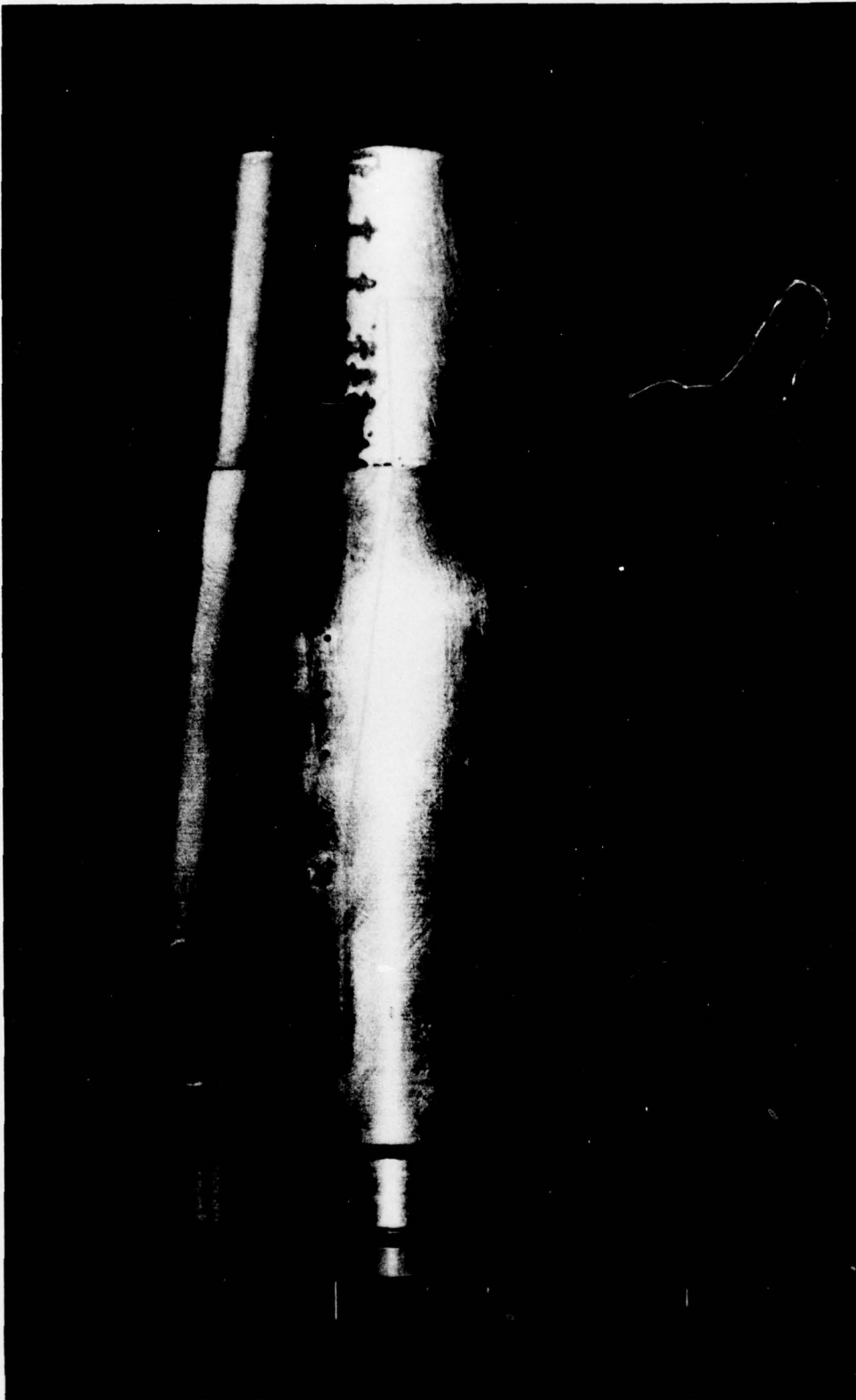
Figure 5. Reheat Nozzle Schematic

Figure 6. Reheat Nozzle

opening was occupied by the support sting. This resulted in a ratio of the sting cross-sectional area to the nozzle throat cross-sectional area of 0.86. A schematic of the cruise nozzle with the support sting and a photograph of the nozzle installed in the wind tunnel are shown in Figures 7 and 8, respectively.

Table 2 contains the important geometric parameters for all nozzles in the free jet and annular jet tests.

Nozzle pressure ratio (ratio of nozzle throat total pressure to free-stream static pressure) was determined by using the average of the pressures measured by three internal total pressure probes located upstream of the nozzle throat.

2. TEST CONDITIONS AND FACILITY DESCRIPTIONS

The free jet nozzle data was obtained in conjunction with the General Dynamics Lightweight Fighter Program. The facility, the Free-Jet Duct Calibration Facility located at General Dynamics, Fort Worth, is shown in schematic in Figure 9. The model was supported in the nine and one quarter inch test section by a forward strut supported hollow sting. Mach number was set by four static pressure orifices in the test section. Nozzle pressure ratio was determined by three total pressure probes in the support shaft. Further facility and experimental data description is included in Reference 1.

The Trisonic Gasdynamics Facility, where the annular sting support was tested, is located at Wright-Patterson Air Force Base. The facility is a closed circuit, variable density continuous flow wind tunnel with an operating Mach range of 0.23 to 3.0. Further facility details are available in Reference 2. Utilizing the solid wall two foot by two foot subsonic test section, the model had a blockage (ratio of the model cross-sectional area to the test section cross-sectional area) of 1.67 percent. A schematic of the annular sting installation in this facility is shown in Figure 10. It will be shown in a later section that the presence of the solid wind tunnel walls did affect the data. For data
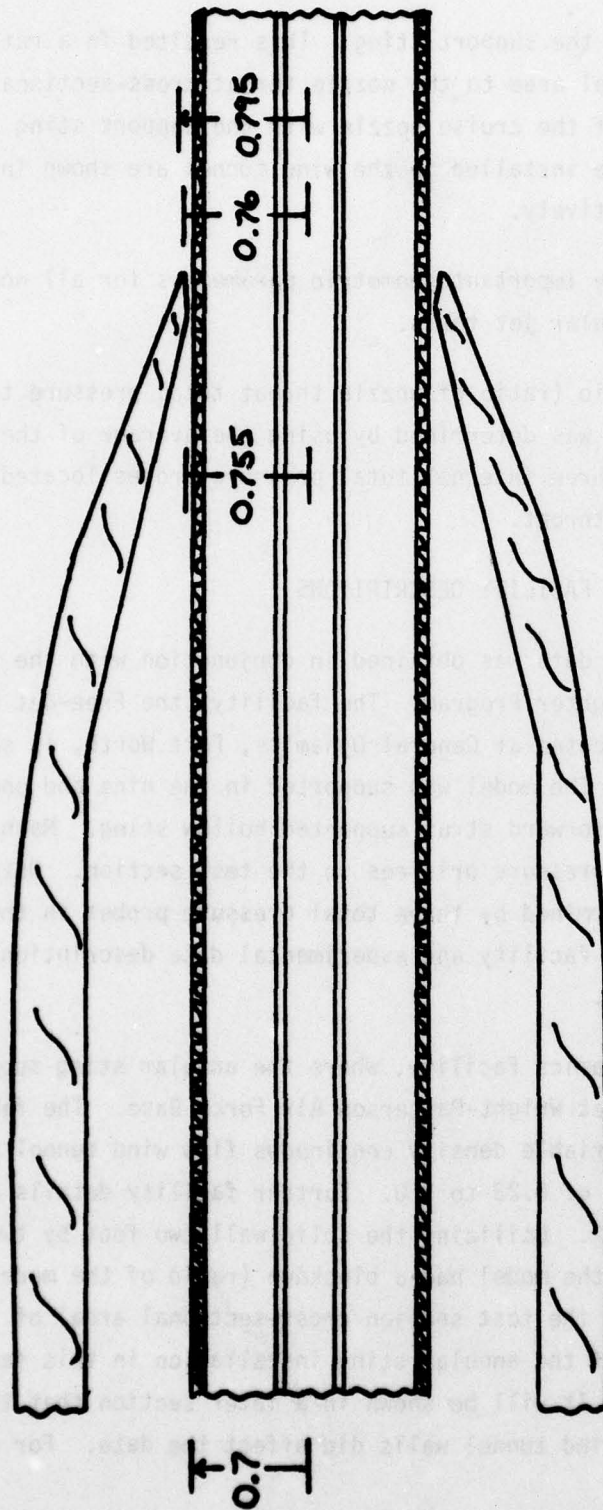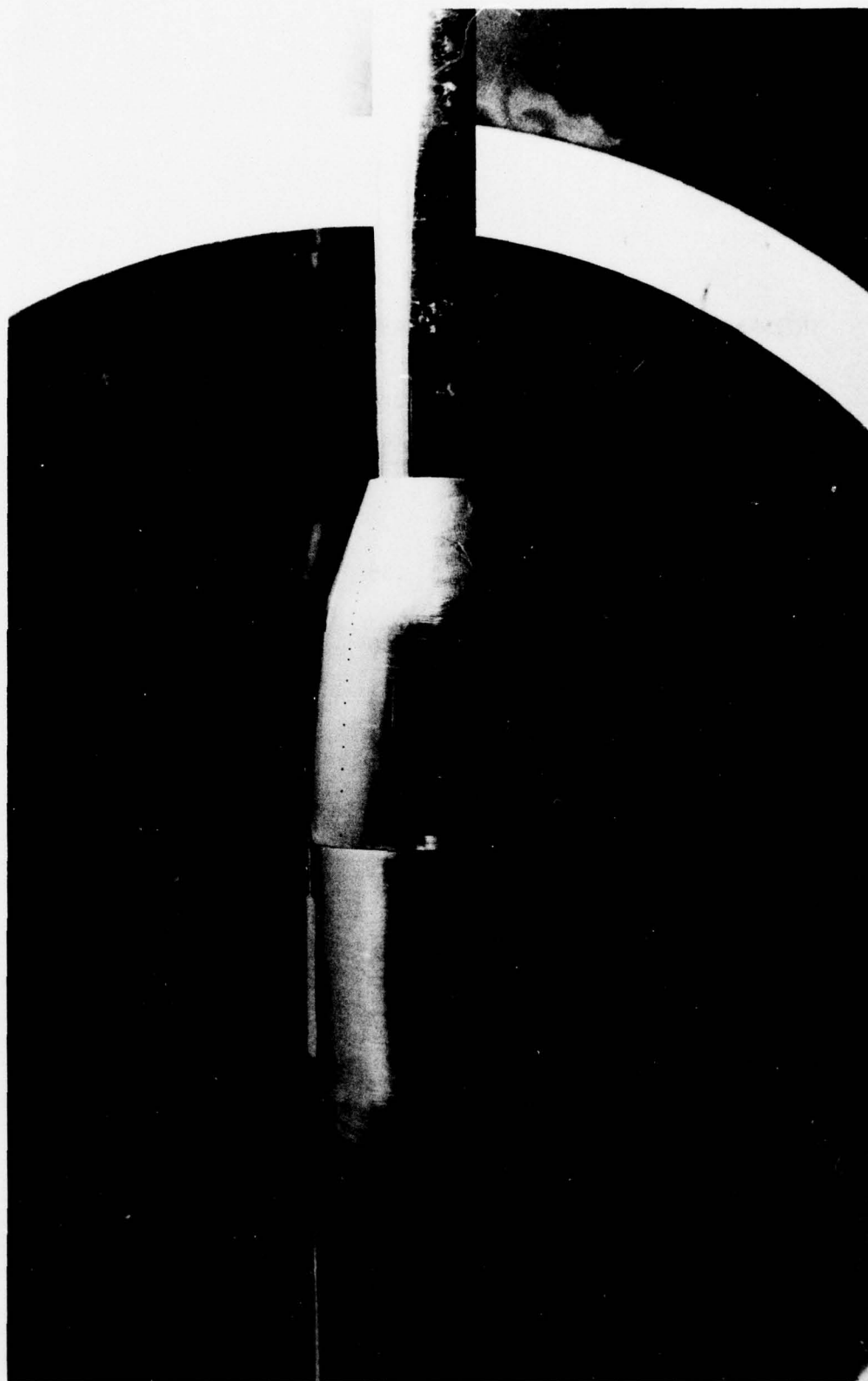
Figure 7. Cruise Nozzle Schematic

Figure 8. Cruise Nozzle

TABLE 2

INTERNAL NOZZLE GEOMETRIC PARAMETERS, FREE JET AND ANNULAR JET

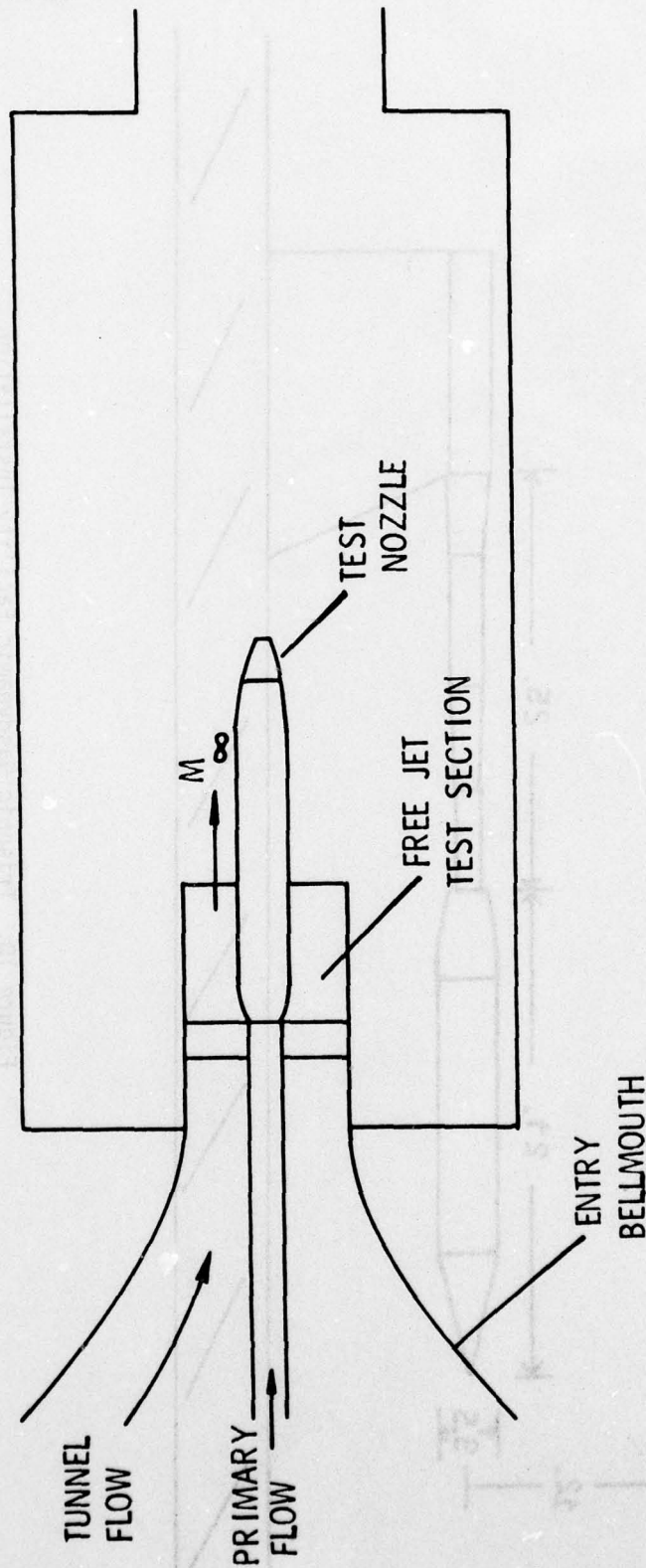| NOZZLE	INTERNAL FLOW AREA RATIO	θ_n	$\dfrac{A_{proj}}{A_{max}}$	$\dfrac{R_{sting}}{R_{throat}}$	$\dfrac{A_{sting}}{A_{throat}}$
Force & Moment					
Annular Jet	1.0	0.0	.36	.698	.487
Free Jet	1.0	0.0	.36	.698	.487
Reheat					
Annular Jet	1.19	2.5	.579	.668	.446
Free Jet	1.19	4.66	.579	--	--
Cruise					
Annular Jet	1.09	1.5	.794	.927	.86
Free Jet	1.09	1.5	.794	--	--

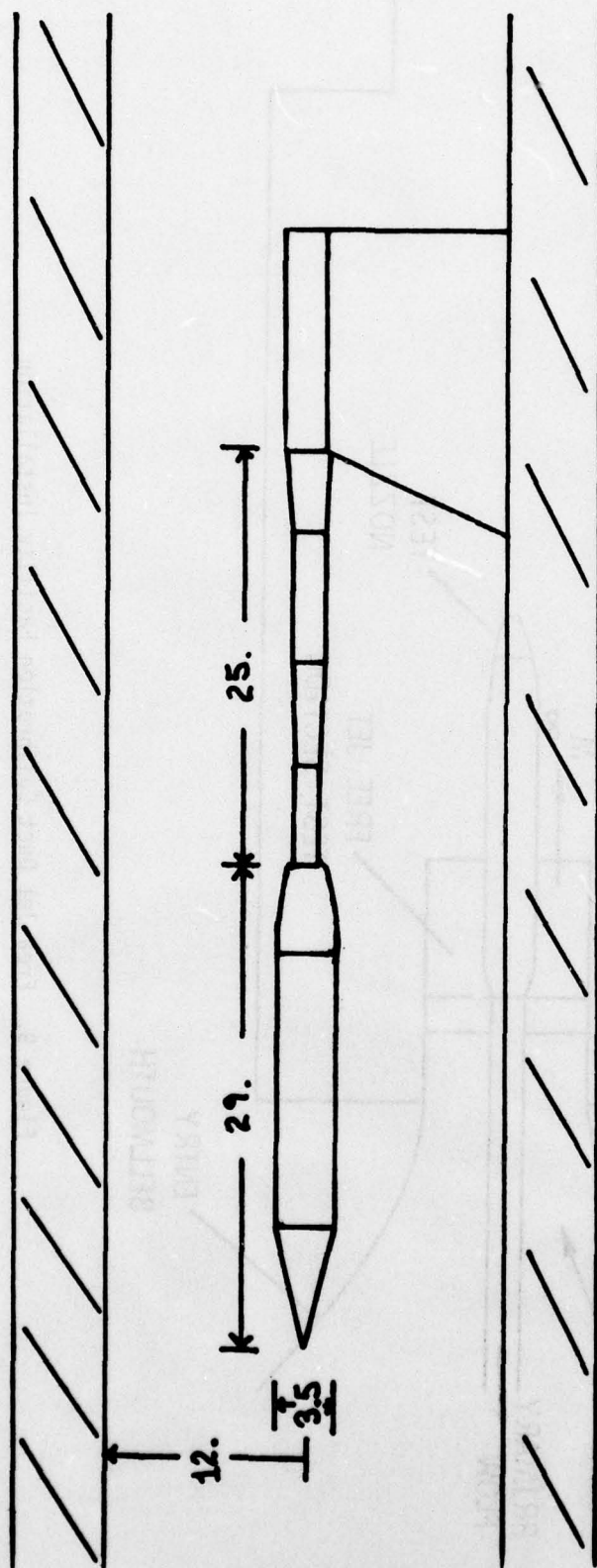Figure 9. Free Jet Duct Calibration Facility Installation

17

Figure 10. Trisonic Gasdynamic Facility Installation

18

comparisons, however, this influence is considered to be negligible.
Direct comparisons of pressure coefficients between the free jet data
from the General Dynamics facility and the annular sting data from the
Air Force Flight Dynamics Laboratory (AFFDL) facility show significant
magnitude differences in the expansion region of the pressure distributions.
These differences may be attributed, in general, to model support differ-
ences and test facility effects. More emphasis will be placed, therefore,
on the ability of the annular sting to simulate jet effects than to
reproduce exactly the free jet data from the Free-Jet Duct Calibration
Facility.

Test Mach numbers were 0.6 and 0.8 at unit Reynolds numbers of 2.0
X 10^6 per foot. Nozzle pressure ratios were simulated from jet-off to
the limit of the test facility high pressure air system. Instrumentation
consisted of the forty-five external nozzle boattail static pressures,
the three internal total pressure probes and schlieren photographs at
selected test conditions.

3. PRESSURE COEFFICIENT DISTRIBUTION COMPARISON-FREE JET AND ANNULAR STING

As discussed previously, the most important task of the annular sting
technique, after verifying that the model can be supported, is to simulate
the jet effects of a free jet. A direct comparison, however, of the
static pressure distributions to verify the jet effects for the free jet
and the annular sting models is compromised by different model mounting
arrangements upstream of the nozzle boattail and different wind tunnel
flow fields. The forward sting mounted free jet model, for example, does
not provide the influence of the cone/cylinder forebody on the aftbody
static pressures. In addition, the finite length cone cylinder model for
the annular sting, due to different wind tunnel Reynolds numbers and
lengths of available boundary layer run, has a boundary layer with
different characteristics than the "infinite" forward sting supported
free jet model. In addition, the proximity of the wind tunnel walls
influences the experimental data for each installation. Due to the
physical arrangement of the experimental apparatus, differences in the
basic static pressure distributions should be expected. No pressure

distributions on the upstream cylindrical section of the model were
available for either testing technique. The source of any pressure dis-
tribution differences, therefore, can not be precisely determined. All
factors previously discussed contribute to these differences. Qualitative
assessments of jet effects, critical to the validation of the annular
sting as a testing technique, are not affected by these variances in
model and wind tunnel facilities.

If the influence of the exhaust jet is eliminated, i.e. tested with
the jet off, the magnitude of these model and facility effects should be
determined. The jet-off pressure coefficient (C_p) is plotted versus dis-
tance from nozzle exit measured forward divided by the nozzle length (X/L)
for the force and moment nozzle as shown in Figure 11. While the static
pressures on the aft cylindrical section of the free jet force and moment
nozzle are limited, the existing pressures in the final boattail region
compare favorably for both the free jet and the annular sting data.
Significant differences in the static pressure distributions in the
initial boattail region are evident for both 0.6 and 0.8 Mach numbers.

The reheat nozzle static pressure coefficient comparisons at jet-off
are shown in Figure 12. As with the force and moment nozzle, the static
pressure distributions for the free jet and the annular sting models com-
pare reasonably well from the aft portion of the nozzle boattail to the
nozzle exit. Significant differences in the initial boattail static
pressure distributions are also evident.

The static pressure coefficient distributions for the cruise nozzle,
presented in Figure 13, indicate large variances throughout the nozzle
boattail region. Those differences in the initial boattail region,
evident for the force and moment and reheat nozzles, may be attributed
to the facility and the upstream model differences discussed previously.
The significant differences in the static pressure coefficient distri-
butions near the nozzle exit, however, may be indicative of a solid body
influence due to the support sting on the annular sting cruise nozzle
boattail. If the support sting is occupying the nozzle exit area as a
flowing jet would, then the effect is to simulate a jet-on condition even
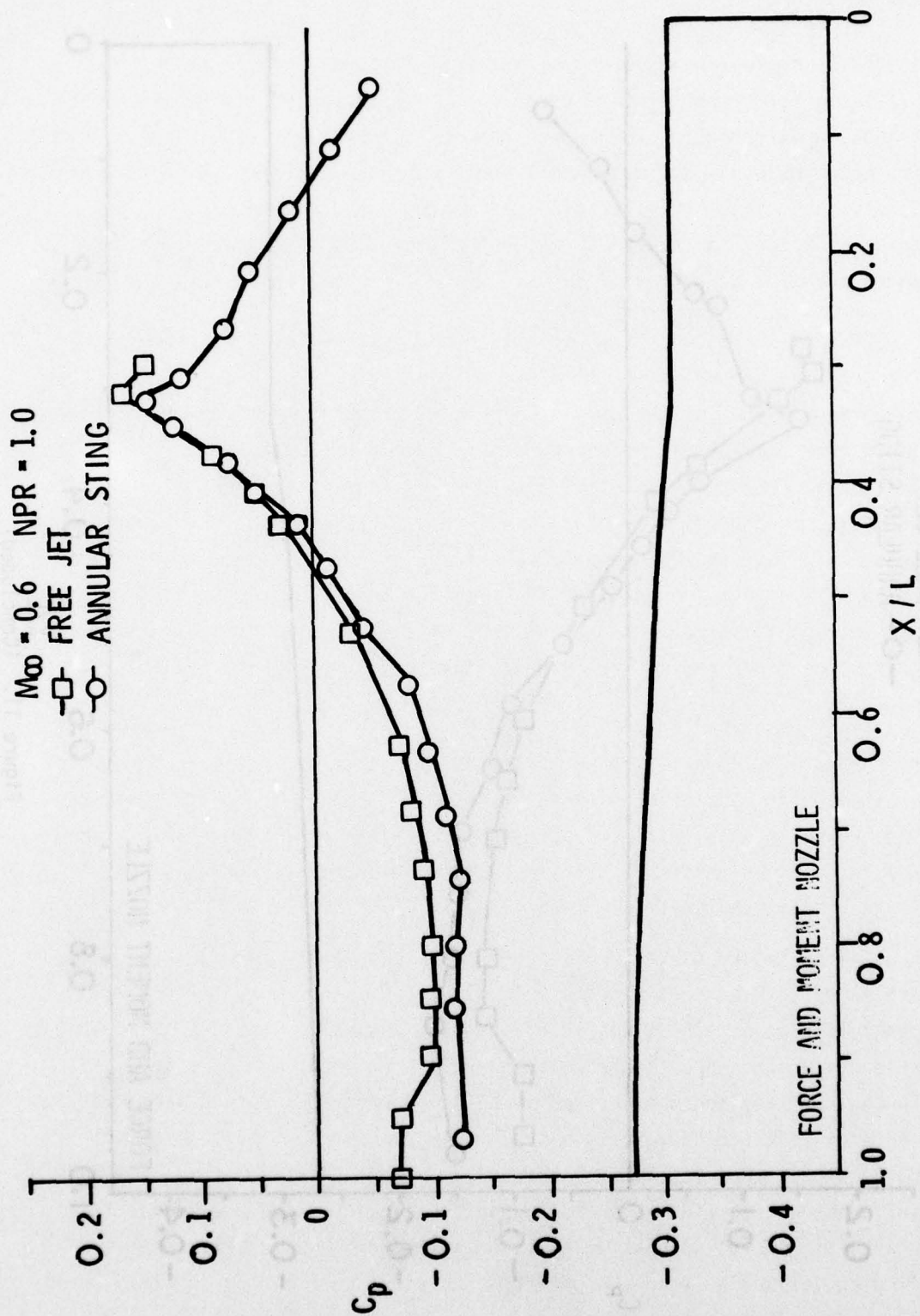at jet-off nozzle pressure ratios.

Figure 11. Force and Moment Nozzle; Free Jet and Annular Sting Jet-Off Pressure Coefficient Distributions
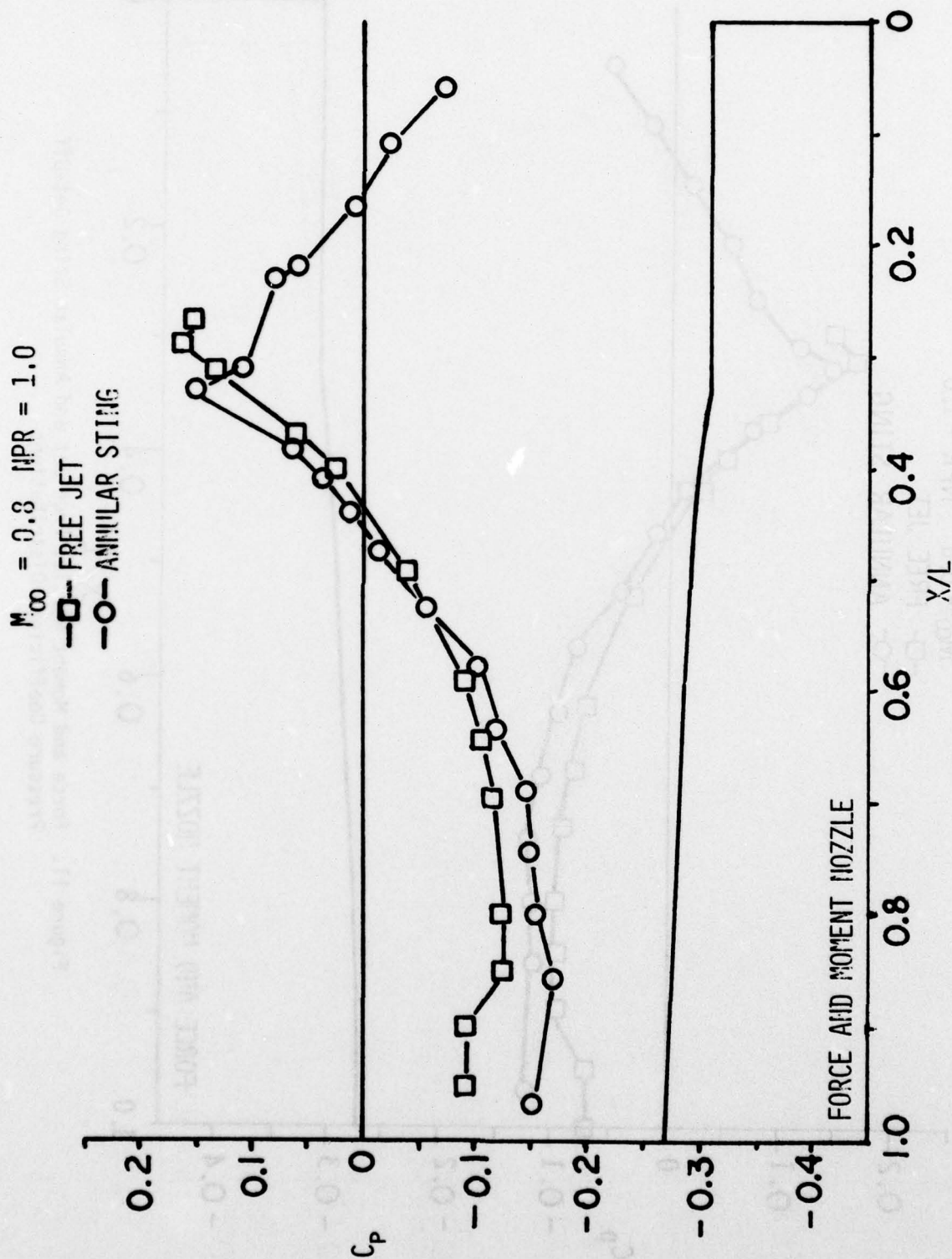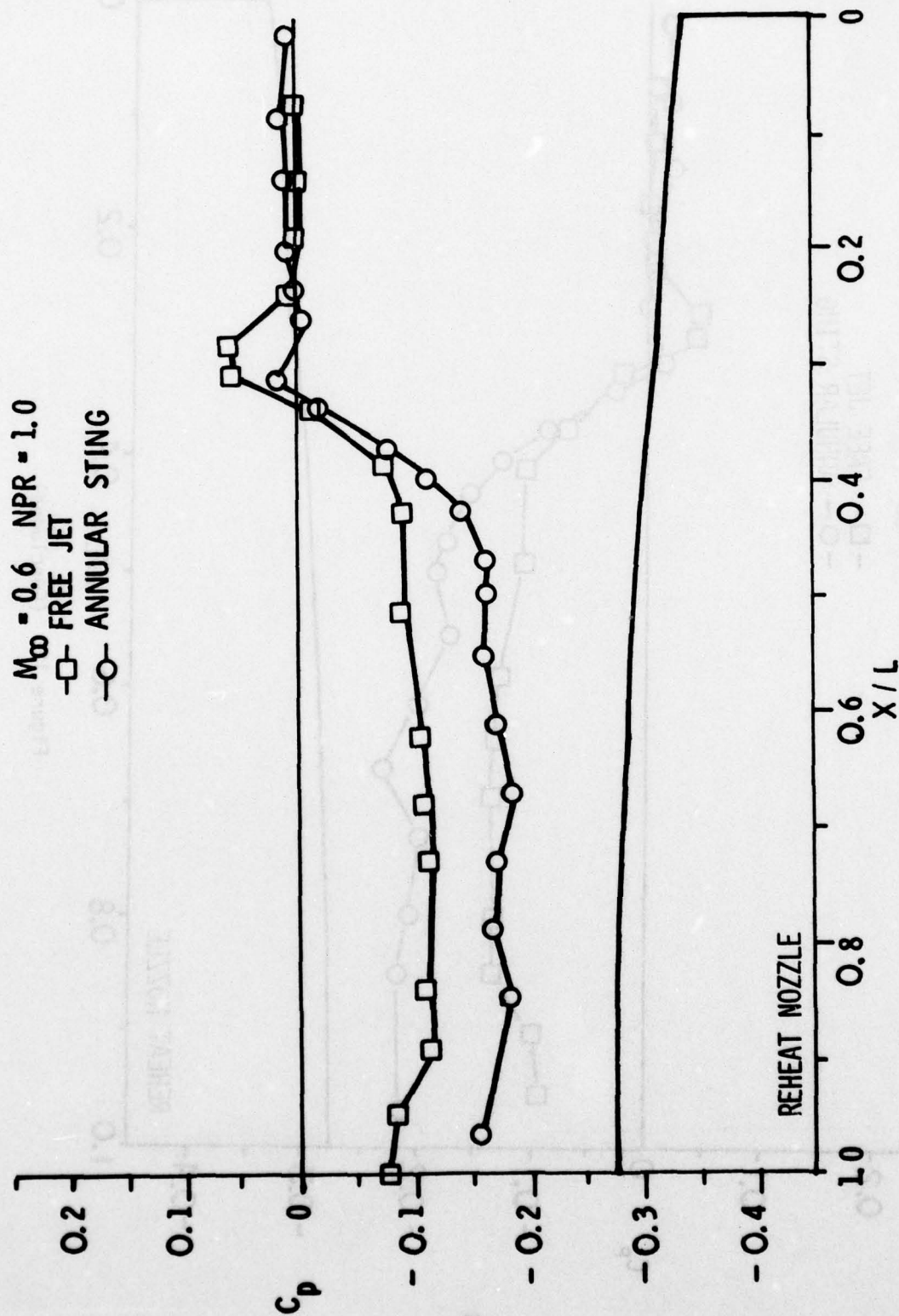
Figure 11. (Concluded)

Figure 12. Reheat Nozzle; Free Jet and Annular Sting Jet-Off Pressure
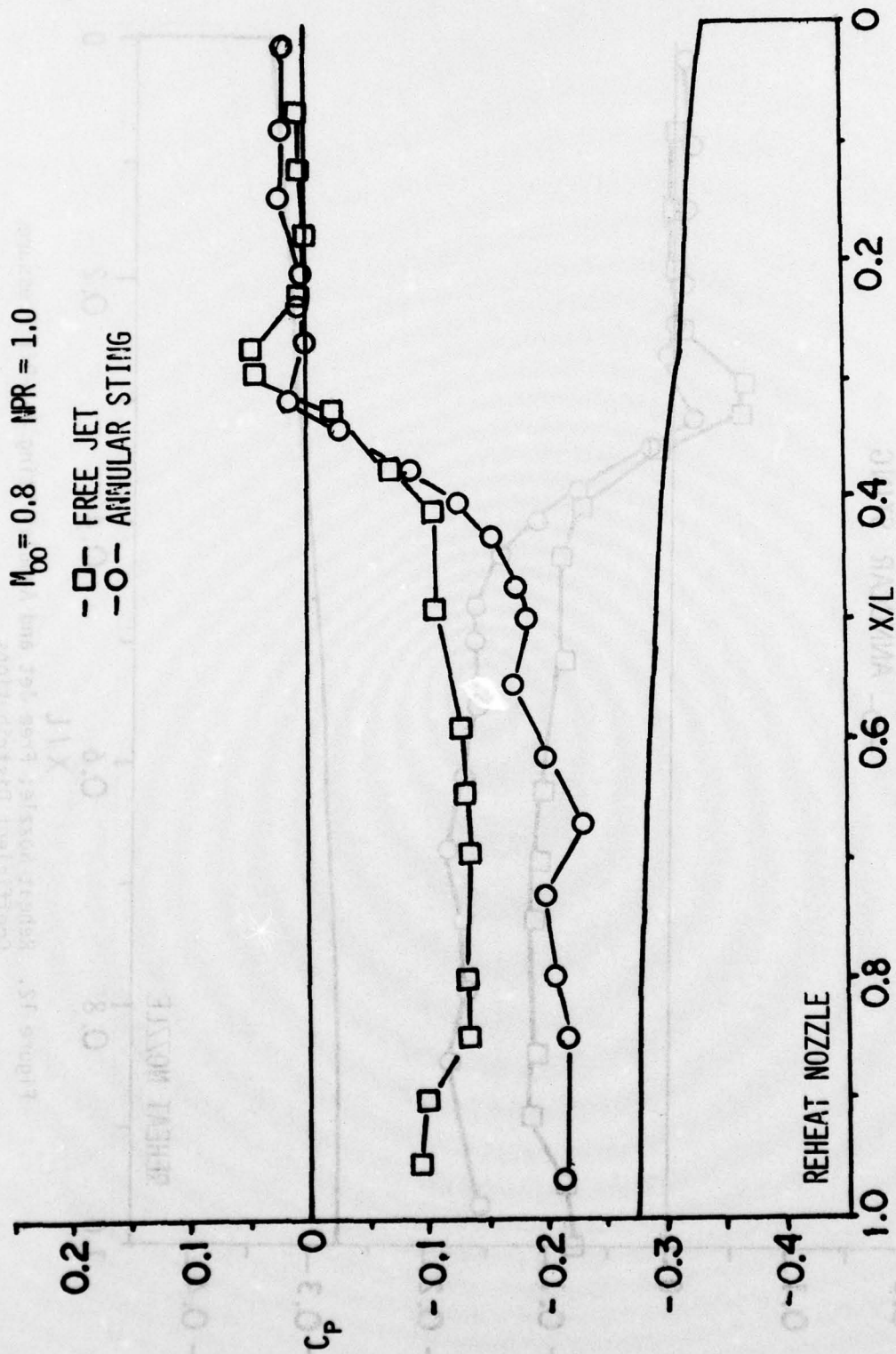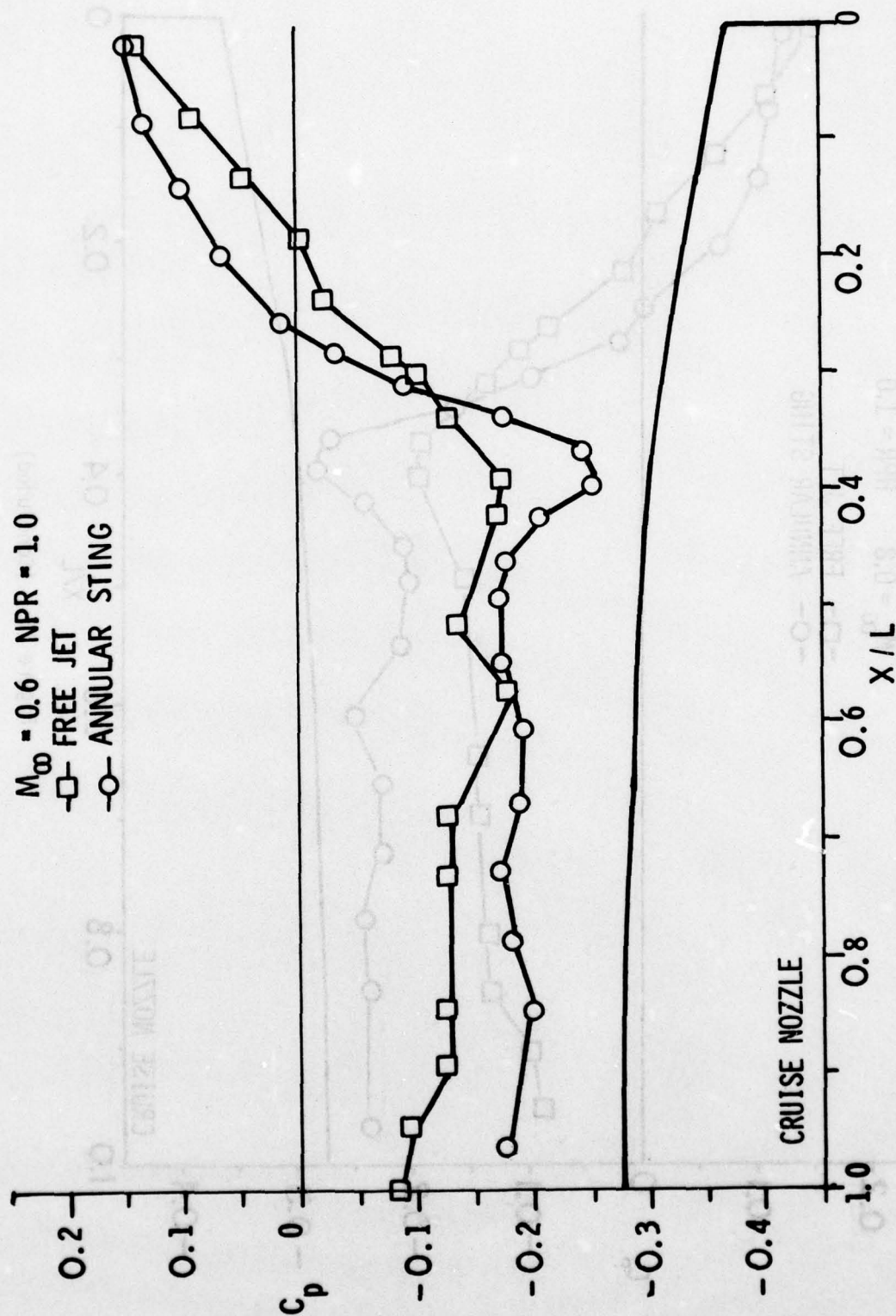Coefficient Distributions

Figure 12. (Concluded)

Figure 13. Cruise Nozzle; Free Jet and Annular Sting Jet-Off Pressure
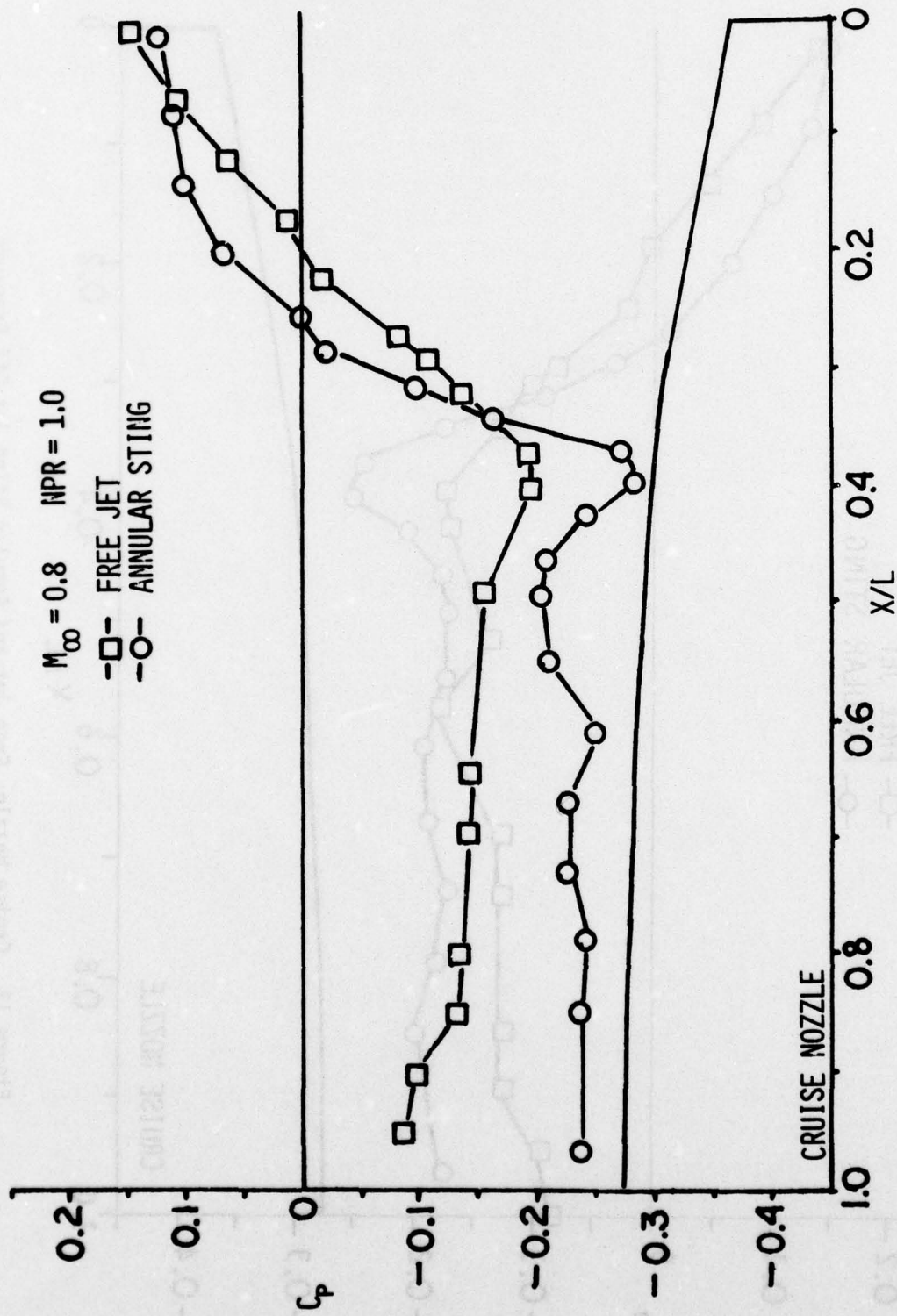Coefficient Distributions

Figure 13. (Concluded)

Comparisons of static pressure distributions for jet-on conditions are shown in Figures 14 and 15. The reheat nozzle at 0.6 and 0.8 Mach number and at a nominal nozzle pressure ratio of 3.0, shows good agreement between the free jet and annular sting pressure distributions from the recompression region aft to the nozzle exit. The differences in the initial boattail region which were present in the jet-off case are also evident here. While the internal nozzle area ratio for the free jet reheat nozzle and the annular sting reheat nozzle were equivalent, the internal nozzle divergence angles for the two testing techniques were not. Using an internal method-of-characteristics program, the initial plume angle for both nozzles was determined as a function of nozzle pressure ratio. When the reheat nozzle pressure distributions for the two testing techniques are compared, therefore, the data used is for nozzle pressure ratios which provide the same initial plume angle for both techniques.

The cruise nozzle static pressure coefficient comparisons at 0.6 and 0.8 Mach numbers and nominal nozzle pressure ratio of 3.0 is shown in Figure 15. While the initial boattail region pressure coefficient differences present in the jet-off data remain when the jet is flowing, relatively good agreement is shown in the recompression region of the nozzle boattail. The pressure coefficient distributions tend to diverge again, however, near the nozzle exit. The solid body influence of the support sting, evident at jet-off, and the small mass flow of the exhaust jet for the annular sting may influence the flow field at the nozzle exit such that the final section of the recompression region is not present. This is the first indication that the support sting for the cruise nozzle may be too large to provide adequate jet effects.

4. JET EFFECTS-FREE JET AND ANNULAR STING

If the annular sting safely supports the nozzle aftbody model in the wind tunnel environment, the major testing requirement then becomes the simulation of jet effects on the nozzle boattail flow field relative to the jet effects of the free jet model. Previous sections have presented areas of suspected solid sting influence which could affect the aftbody flow field. The cruise nozzle data also indicates incomplete recompression
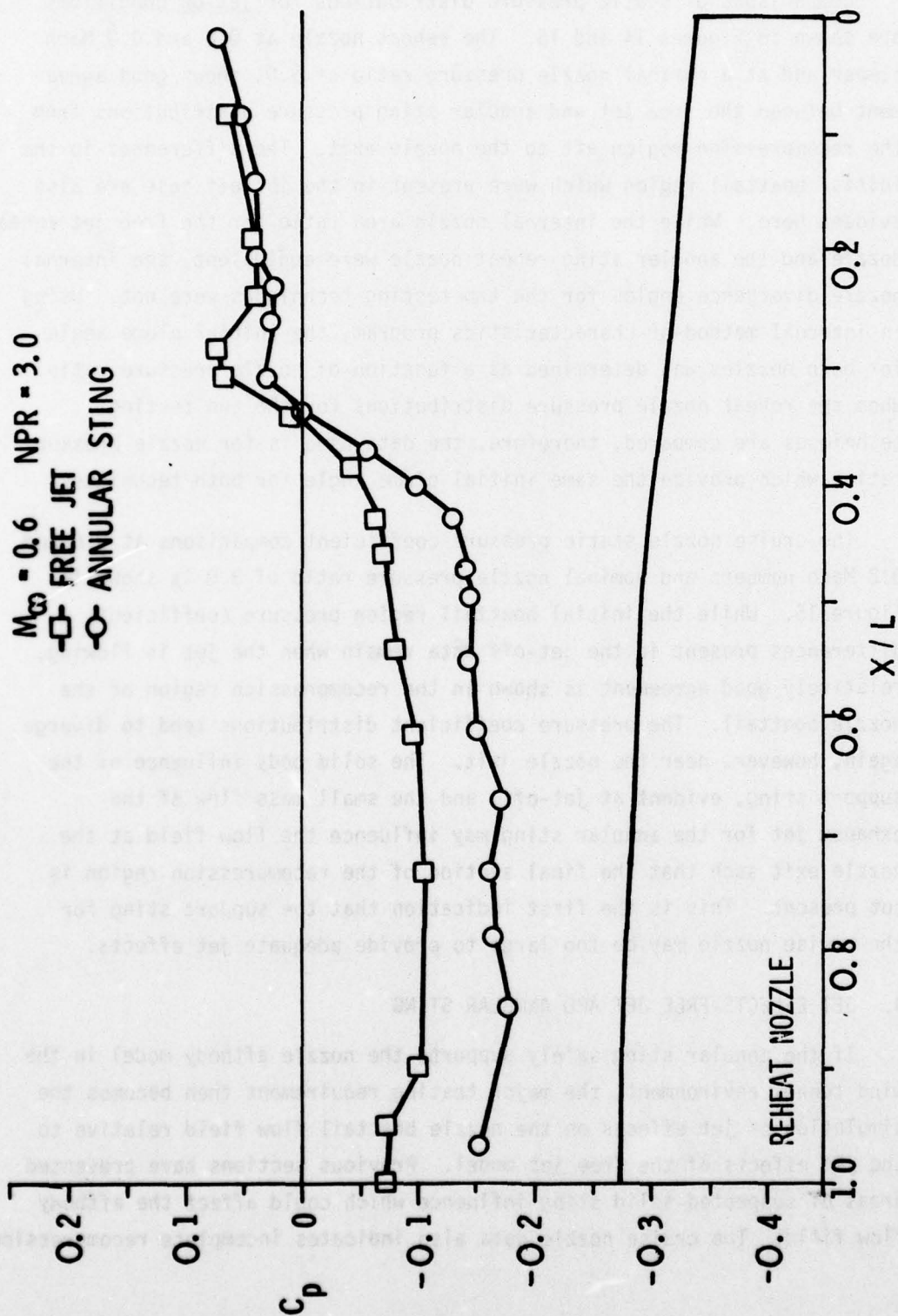
Figure 14.   Reheat Nozzle; Free Jet and Annular Sting NPR=3.0 Pressure
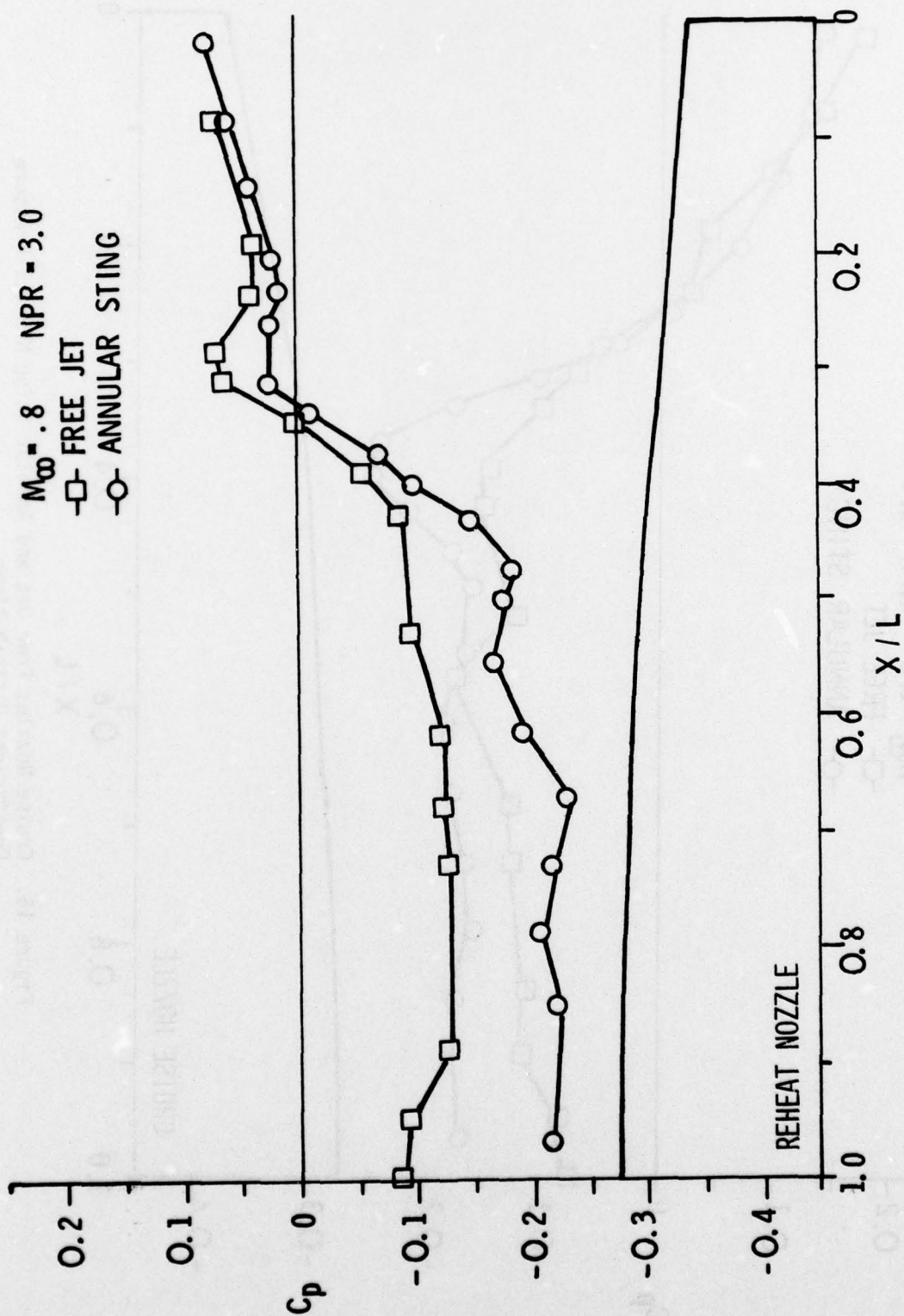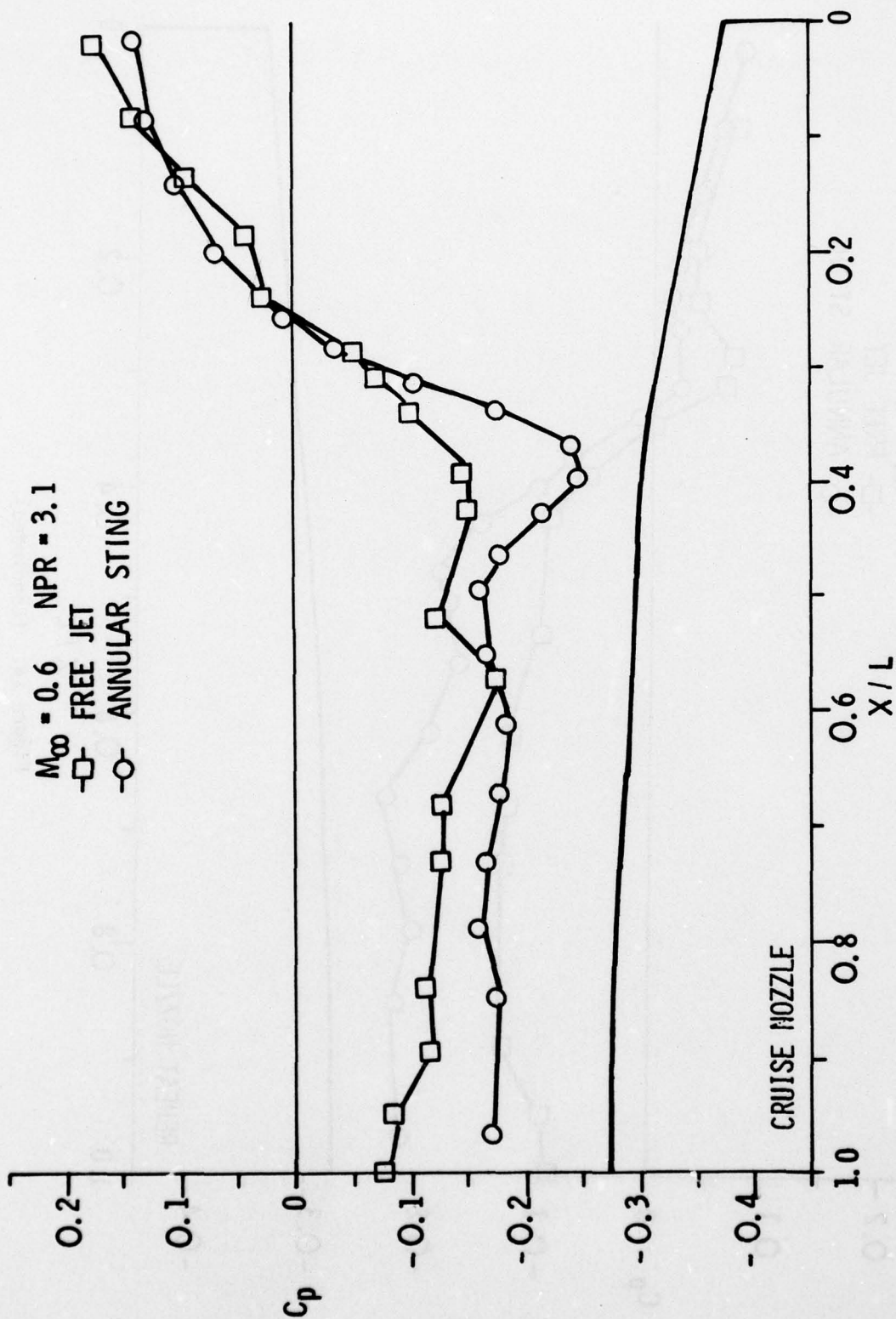Coefficient Distributions

Figure 14. (Concluded)

Figure 15. Cruise Nozzle; Free Jet and Annular Sting NPR=3.1 Pressure Coefficient Distributions
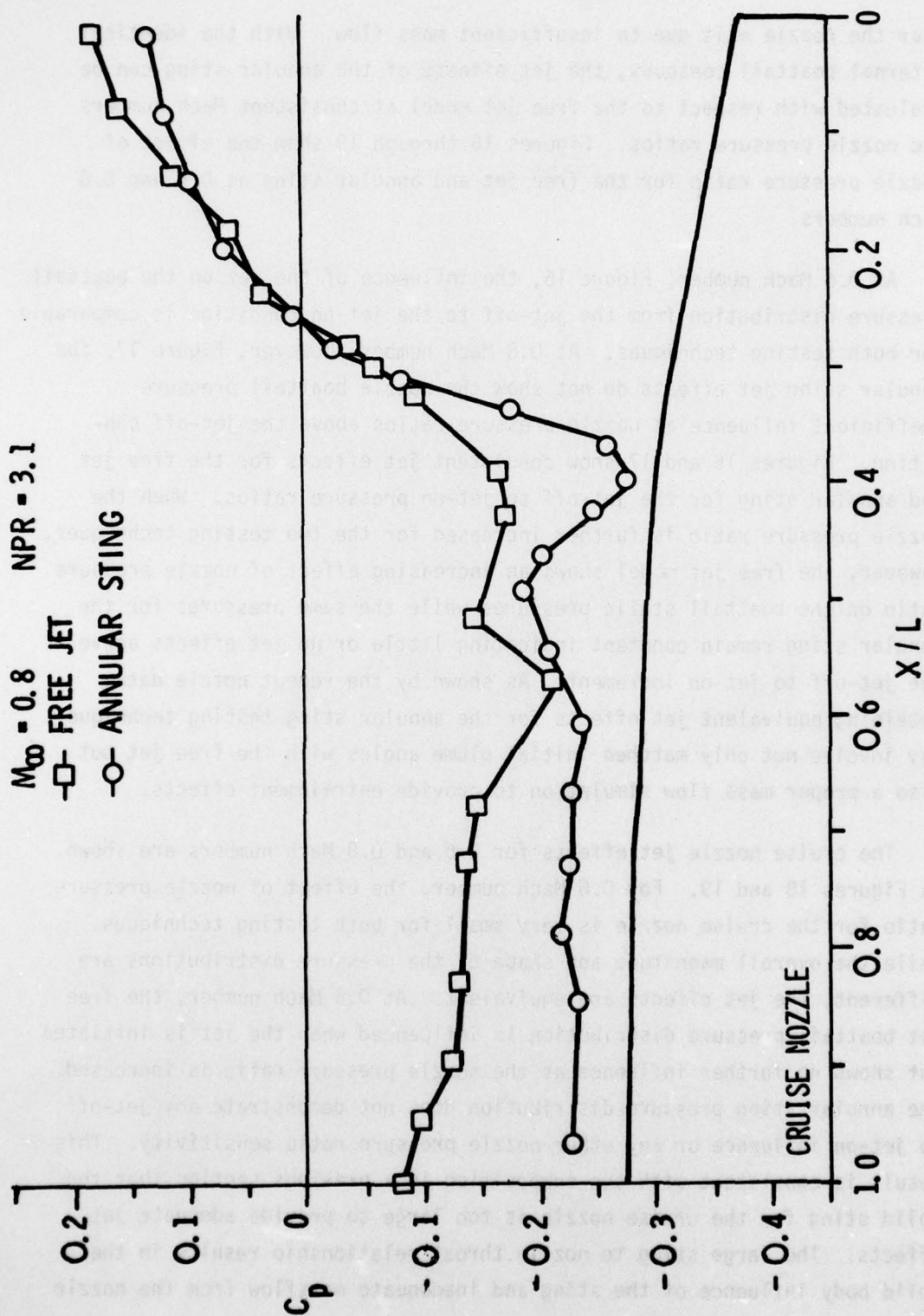
Figure 15. (Concluded)

near the nozzle exit due to insufficient mass flow. With the identical
external boattail contours, the jet effects of the annular sting can be
evaluated with respect to the free jet model at consistent Mach numbers
and nozzle pressure ratios. Figures 16 through 19 show the effect of
nozzle pressure ratio for the free jet and annular sting at 0.6 and 0.8
Mach numbers.

At 0.6 Mach number, Figure 16, the influence of the jet on the boattail
pressure distribution from the jet-off to the jet-on condition is comparable
for both testing techniques. At 0.8 Mach number, however, Figure 17, the
annular sting jet effects do not show the nozzle boattail pressure
coefficient influence at nozzle pressure ratios above the jet-off con-
dition. Figures 16 and 17 show consistent jet effects for the free jet
and annular sting for the jet-off to jet-on pressure ratios. When the
nozzle pressure ratio is further increased for the two testing techniques,
however, the free jet model shows an increasing effect of nozzle pressure
ratio on the boattail static pressures while the same pressures for the
annular sting remain constant indicating little or no jet effects above
the jet-off to jet-on increment. As shown by the reheat nozzle data,
obtaining equivalent jet effects for the annular sting testing technique
may involve not only matched initial plume angles with the free jet but
also a proper mass flow simulation to provide entrainment effects.

The cruise nozzle jet effects for 0.6 and 0.8 Mach numbers are shown
in Figures 18 and 19. For 0.6 Mach number, the effect of nozzle pressure
ratio for the cruise nozzle is very small for both testing techniques.
While the overall magnitude and shape of the pressure distributions are
different, the jet effects are equivalent. At 0.8 Mach number, the free
jet boattail pressure distribution is influenced when the jet is initiated
but shows no further influence as the nozzle pressure ratio is increased.
The annular sting pressure distribution does not demonstrate any jet-off
to jet-on influence or any other nozzle pressure ratio sensitivity. This
result is consistent with the supposition in a previous section that the
solid sting for the cruise nozzle is too large to provide adequate jet
effects. The large sting to nozzle throat relationship results in the
solid body influence of the sting and inadequate massflow from the nozzle
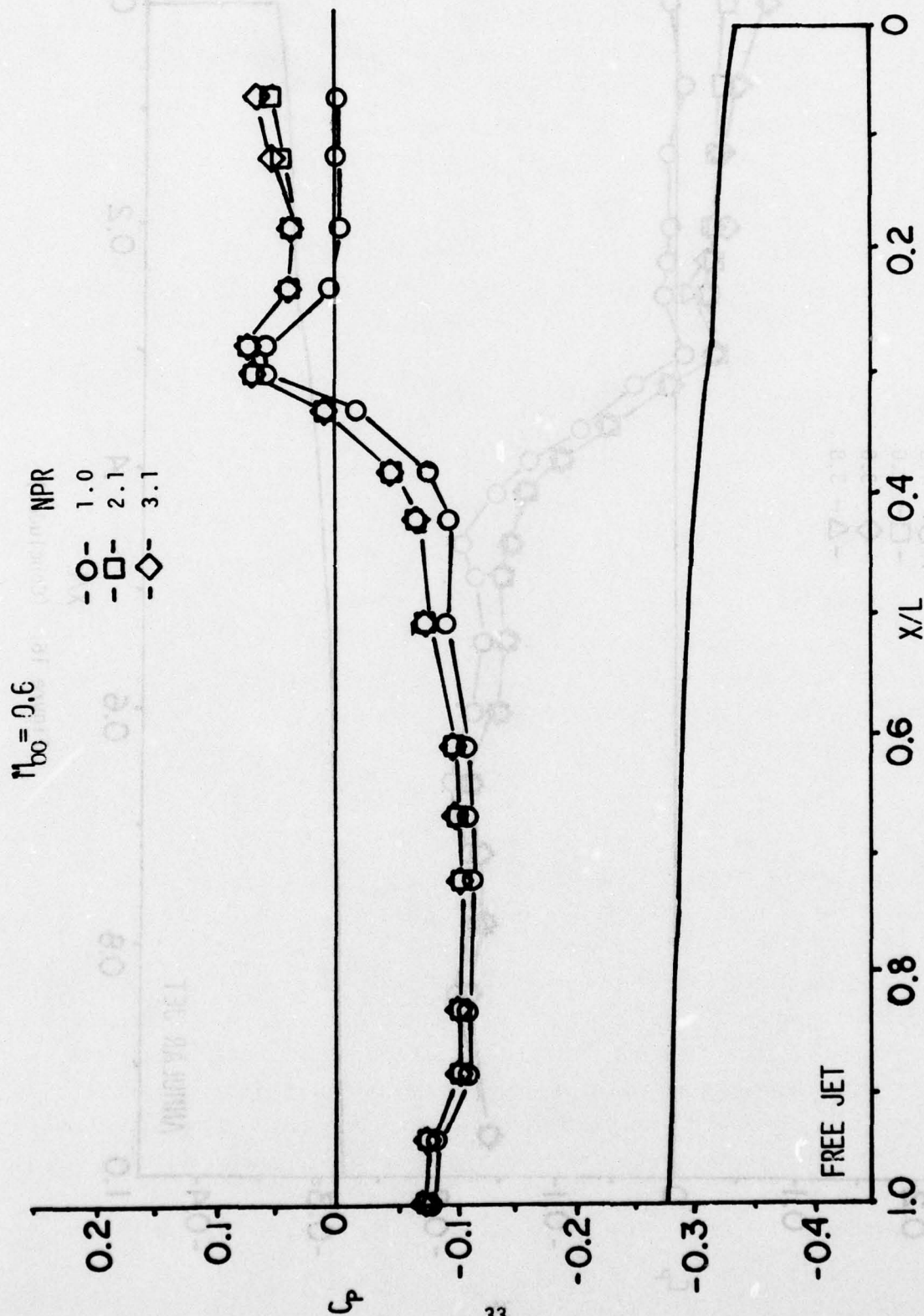exit.

Figure 16.   Reheat Nozzle; Free Jet and Annular Sting Nozzle Pressure
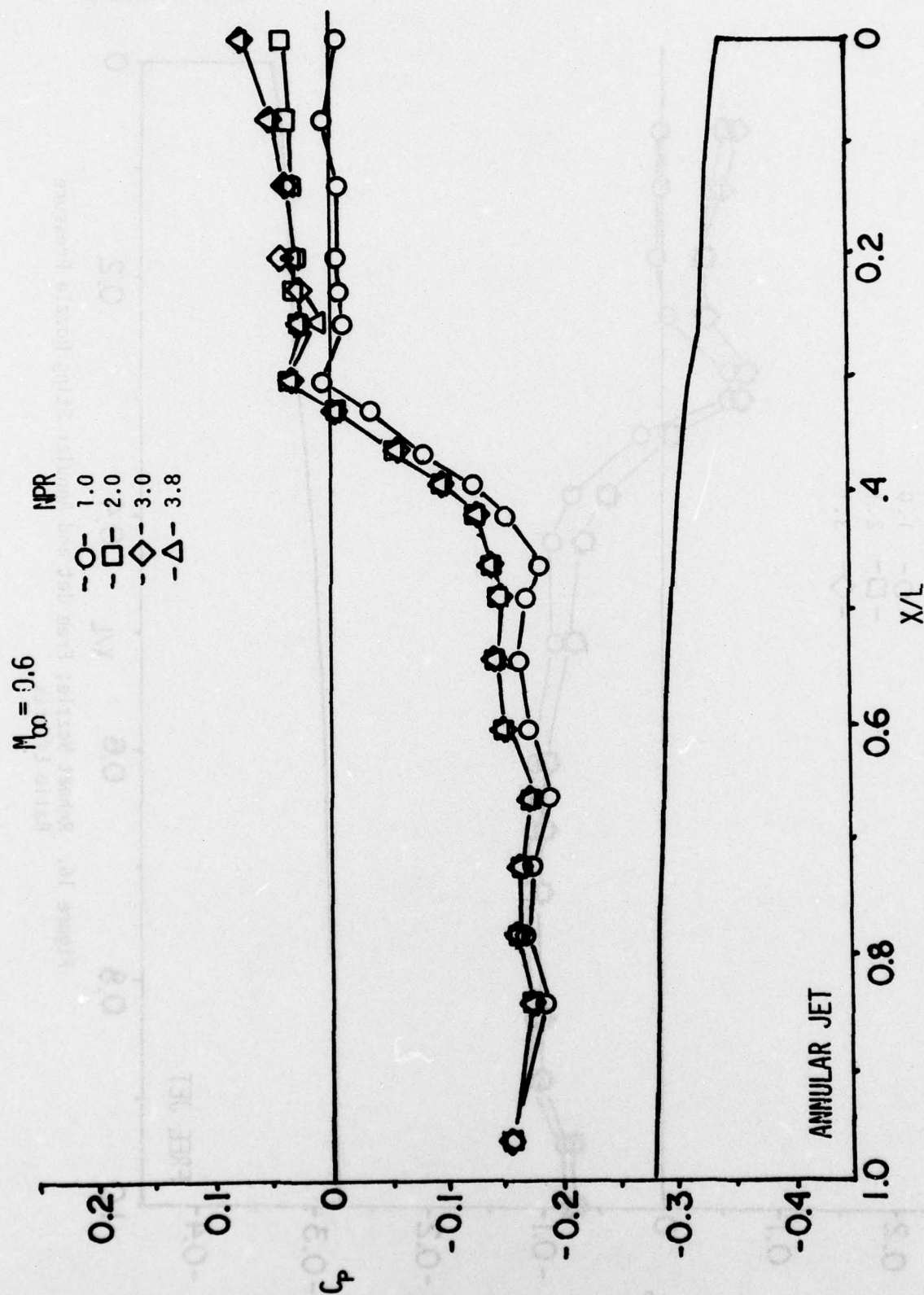Ratio Effects
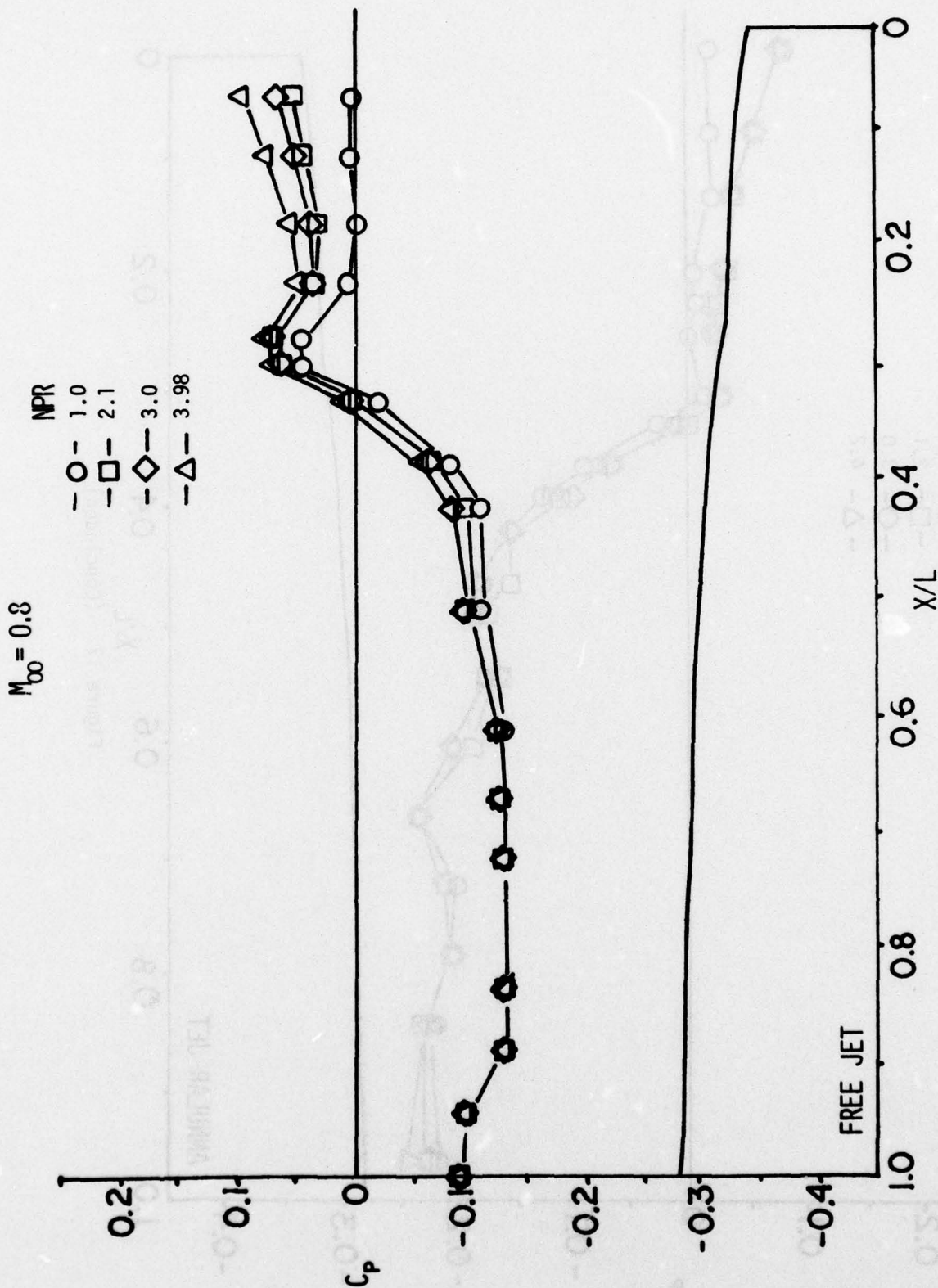
Figure 16. (Concluded)

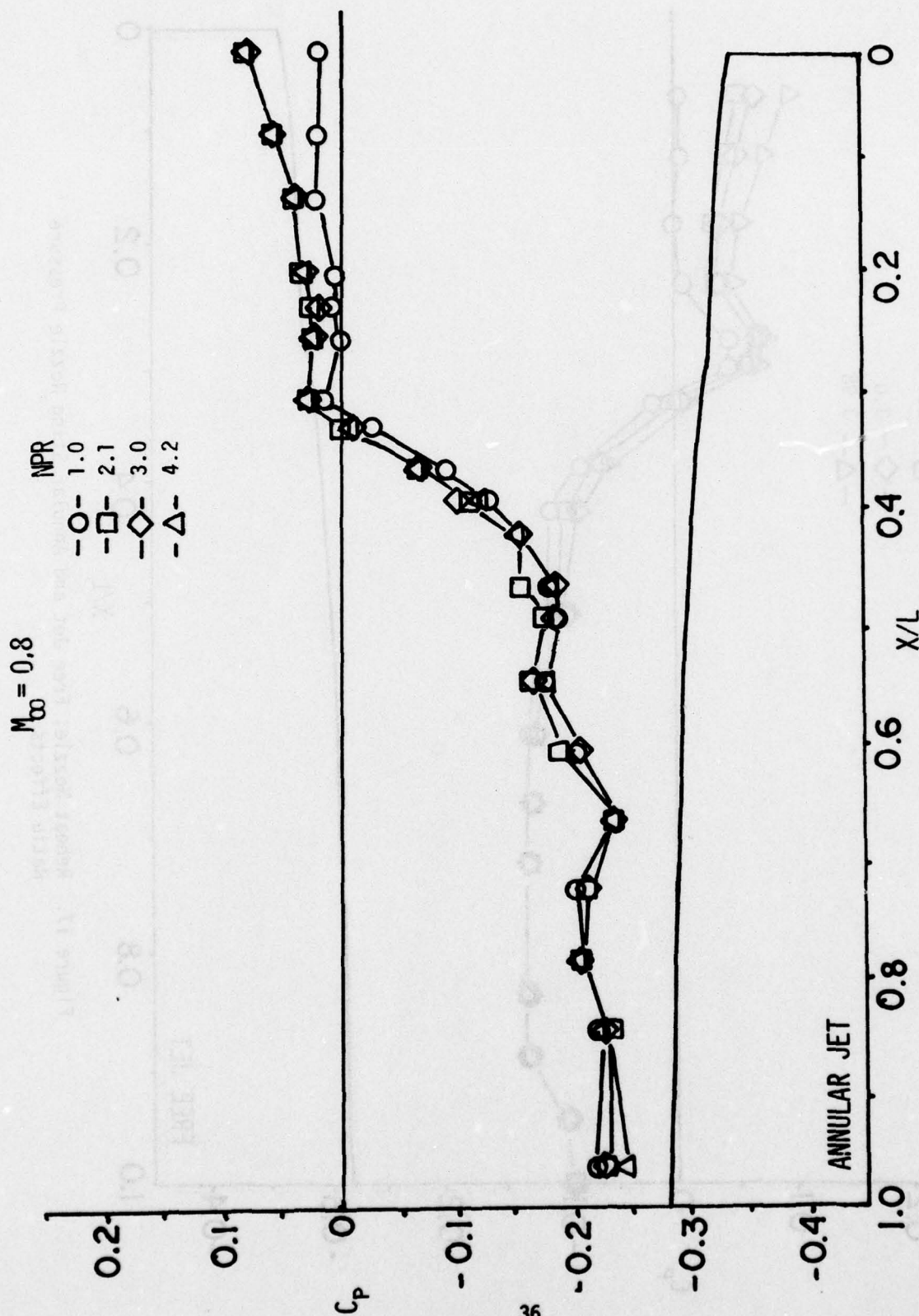Figure 17. Reheat Nozzle; Free Jet and Annular Sting Nozzle Pressure Ratio Effects
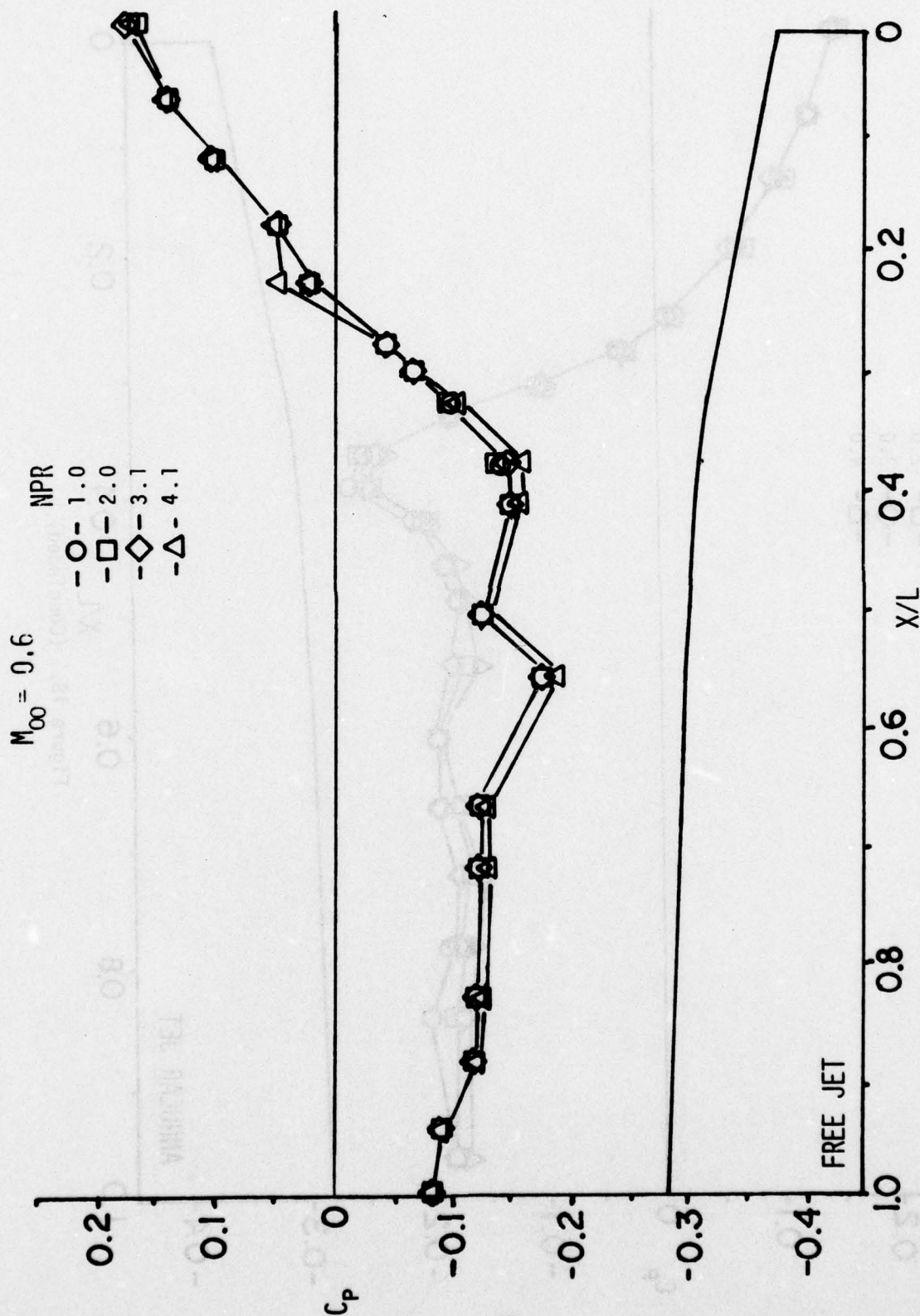
Figure 17. (Concluded)

Figure 18. Cruise Nozzle; Free Jet and Annular Sting Nozzle Pressure Ratio Effects
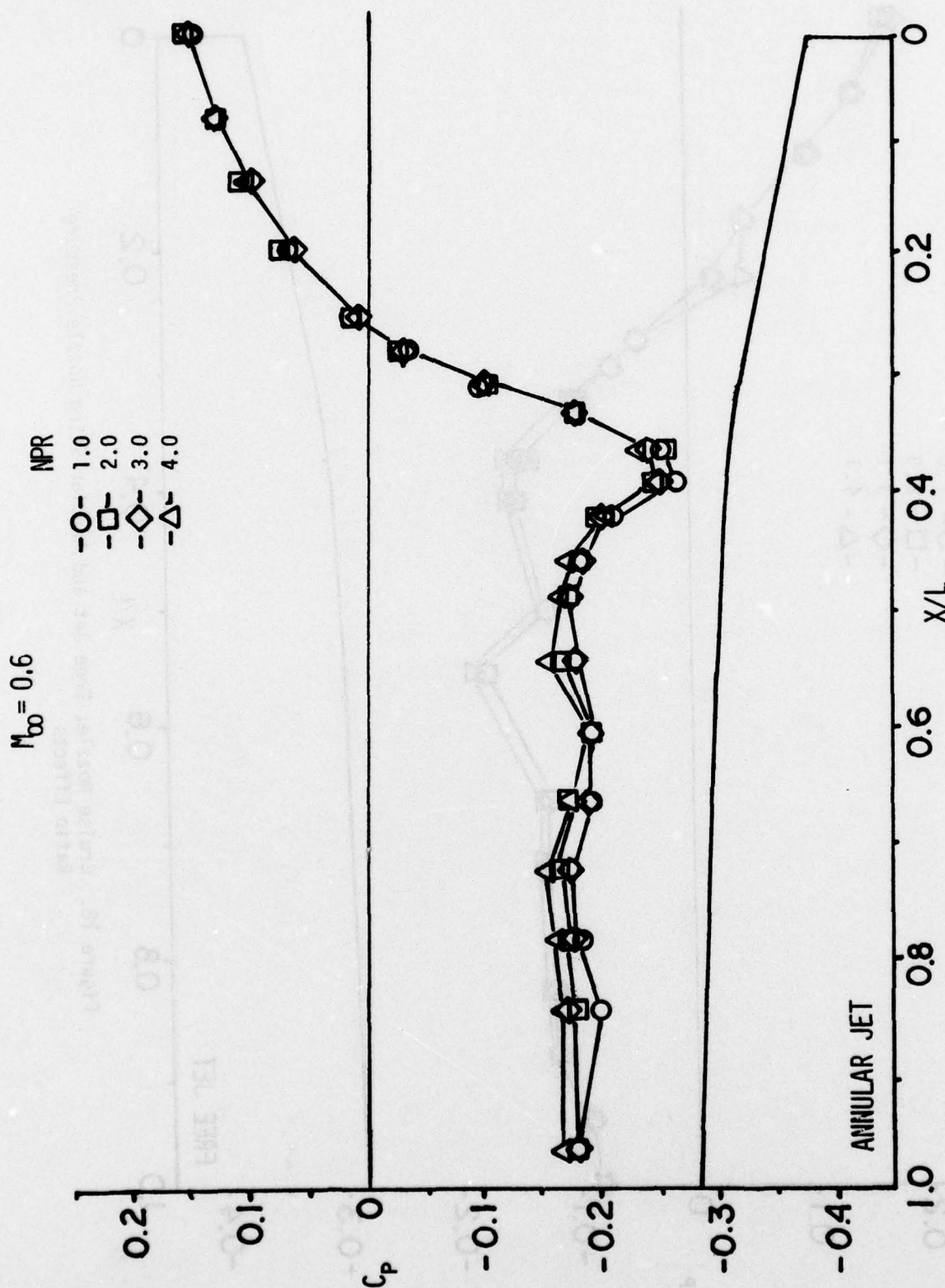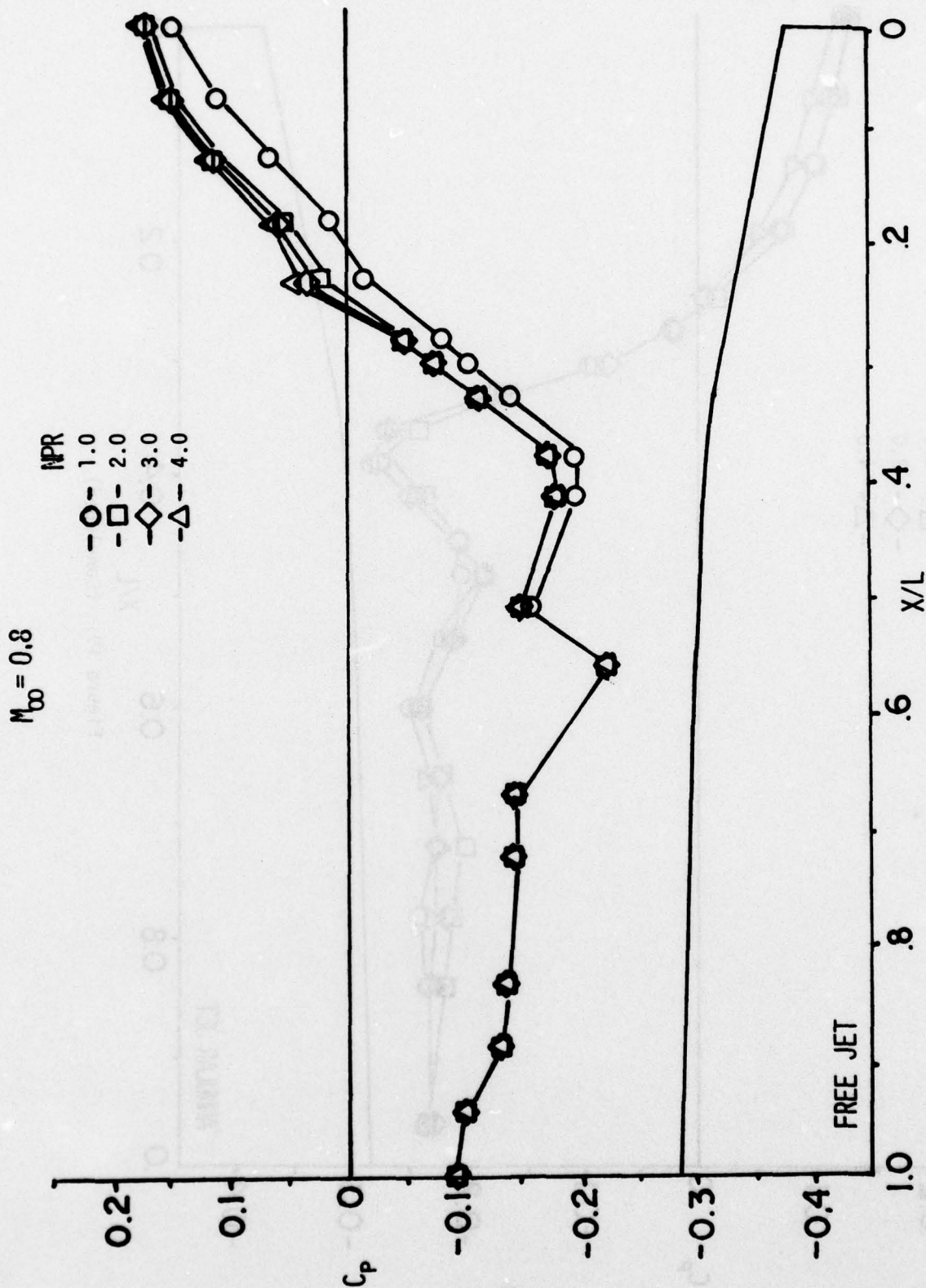
Figure 18. (Concluded)

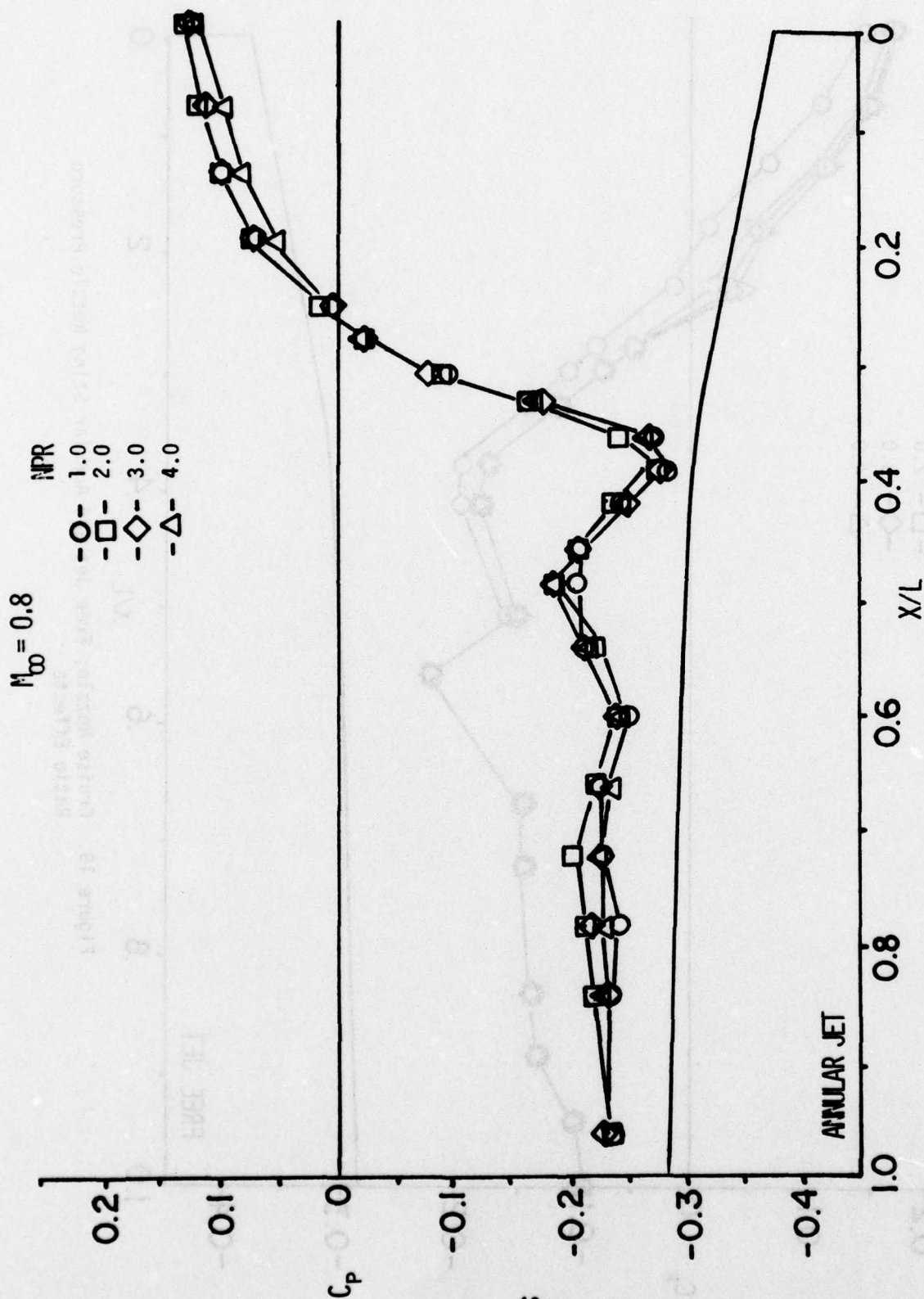Figure 19. Cruise Nozzle; Free Jet and Annular Sting Nozzle Pressure Ratio Effects

Figure 19. (Concluded)

For this annular sting apparatus, the reheat nozzle appears to simulate most of the free jet nozzle pressure ratio effects and safely supports the wind tunnel model. The cruise nozzle shows only limited jet effects when compared to the free jet model. From both nozzles it is evident that sufficient massflow must be provided at the nozzle exit to simulate the jet-off to jet-on influence on the boattail pressures as well as the effect of increasing nozzle pressure ratio. Proper simulation of the jet effects is critical if the annular sting support is to be suitable as an aftbody nozzle testing technique. The relationship of nozzle throat flow area, support sting diameter, and nozzle massflow requires further evaluation to devise optimum annular sting test apparatus to satisfy both requirements of model support and adequate jet effects.

5. EXHAUST PLUME CONTOURS-FREE JET AND ANNULAR STING

Exhaust nozzles with equivalent internal geometric characteristics tested at the same nozzle pressure ratio will have identical initial plume angles. Downstream of the nozzle exit, however, the character of the exhaust plume may be drastically altered if, for example, a support sting is introduced. Subsonically, the geometric character of the plume will influence the flow field upstream of the exhaust plume and consequently will affect the nozzle boattail pressure distribution. Using an internal method-of-characteristics computer program, the exhaust plume boundaries of both the free jet and annular sting models were calculated and then compared to schlieren photographs taken during the annular sting test. Comparing the exhaust plume contours for the two testing techniques may qualitatively indicate further potential sources of the flow field differences present in the boattail static pressure coefficient distributions.

The calculated plume contours for the reheat nozzle for 0.6 and 0.8 Mach numbers at a nominal nozzle pressure ratio of 5.0 is presented in Figure 20. For the same initial plume angle, the annular sting nozzle has almost two plume wavelengths for every one wavelength for the free jet. This two-to-one relation for annular sting to free jet wavelengths
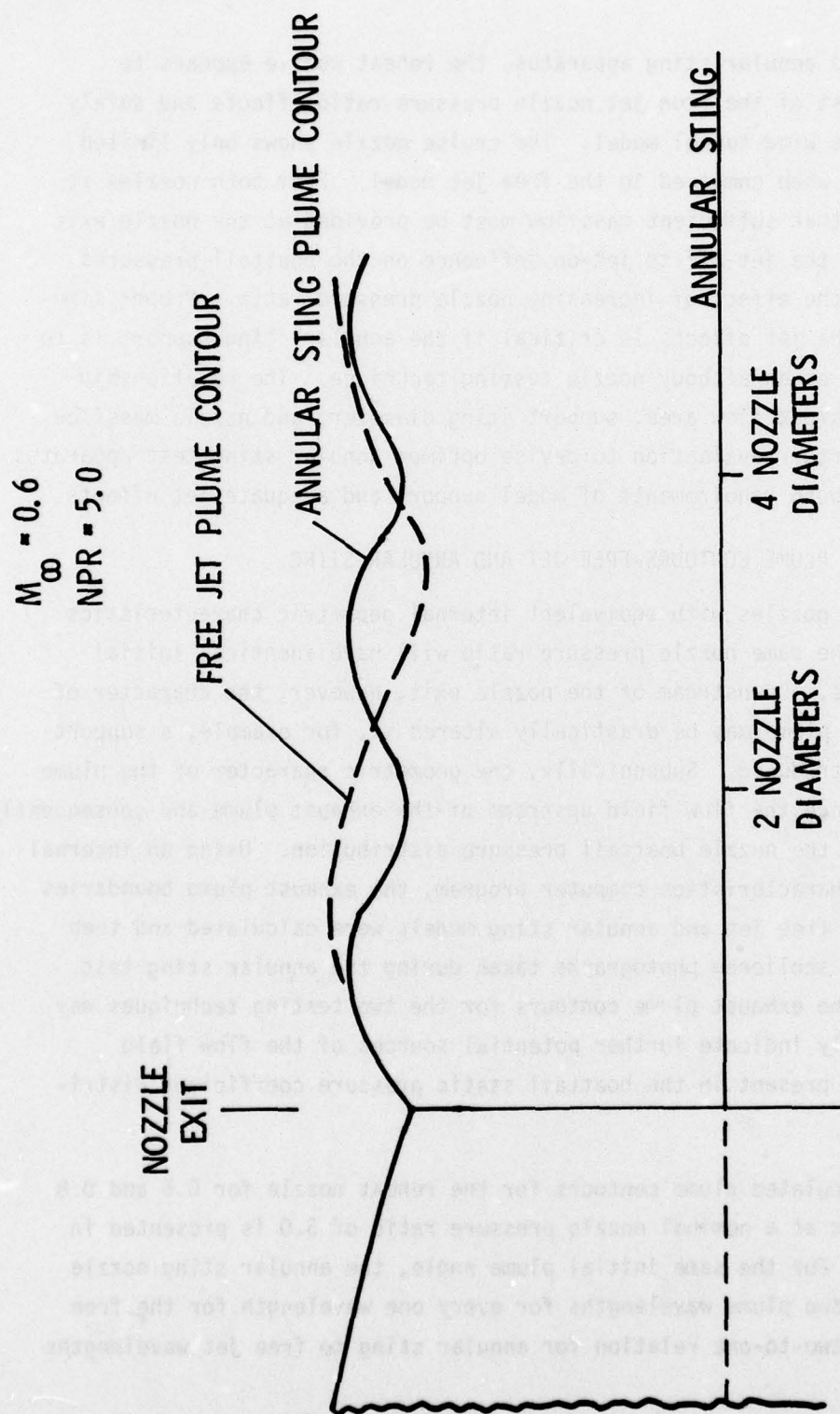
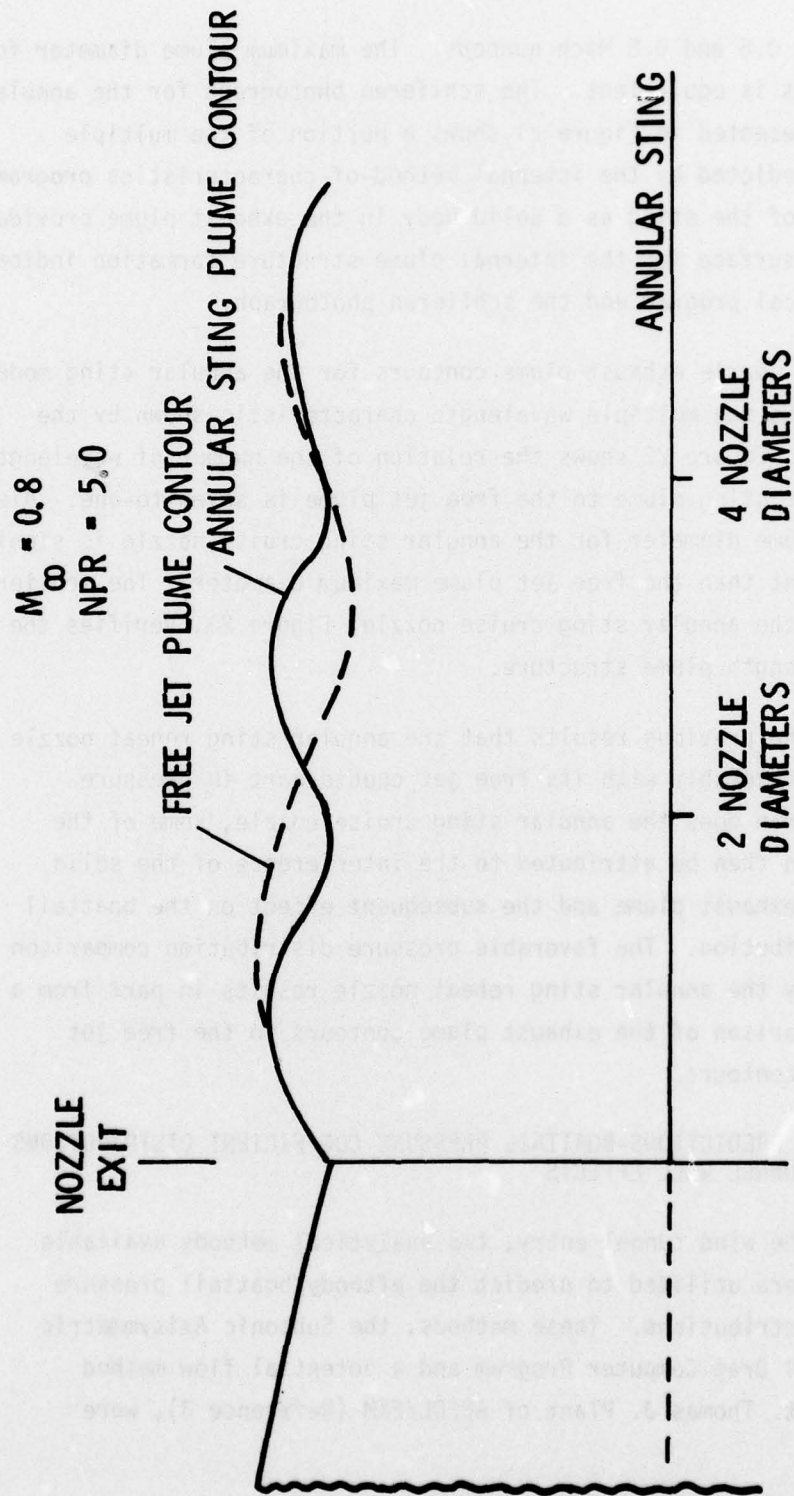Figure 20. Reheat Nozzle; Free Jet and Annular Sting Plume Contours

NOZZLE
EXIT

FREE JET PLUME CONTOUR

ANNULAR STING PLUME CONTOUR

ANNULAR STING

$M_\infty = 0.8$
NPR = 5.0

2 NOZZLE
DIAMETERS

4 NOZZLE
DIAMETERS

Figure 20. (Concluded)

43

holds for both 0.6 and 0.8 Mach numbers. The maximum plume diameter for both techniques is equivalent. The schlieren photograph for the annular sting model presented in Figure 21 shows a portion of the multiple wavelengths predicted by the internal method-of-characteristics program. The proximity of the sting as a solid body in the exhaust plume provides the necessary surface for the internal plume structure formation indicated by the analytical program and the schlieren photograph.

The cruise nozzle exhaust plume contours for the annular sting model also demonstrate the multiple wavelength characteristic shown by the reheat nozzle. Figure 22 shows the relation of the number of wavelengths for the annular sting plume to the free jet plume is seven-to-one. Also the maximum plume diameter for the annular sting cruise nozzle is significantly different than the free jet plume maximum diameter. The schlieren photograph of the annular sting cruise nozzle, Figure 23, verifies the multiple wavelength plume structure.

Based on the previous results that the annular sting reheat nozzle compares more favorably with its free jet counterpart in pressure distribution than does the annular sting cruise nozzle, some of the differences can then be attributed to the interference of the solid sting and the exhaust plume and the subsequent effect on the boattail pressure distribution. The favorable pressure distribution comparison demonstrated by the annular sting reheat nozzle results in part from a favorable comparison of the exhaust plume contours to the free jet exhaust plume contours.

6. ANALYTICAL PREDICTIONS-BOATTAIL PRESSURE COEFFICIENT DISTRIBUTIONS AND WIND TUNNEL WALL EFFECTS

Prior to the wind tunnel entry, two analytical methods available in the AFFDL were utilized to predict the aftbody/boattail pressure coefficient distributions. These methods, the Subsonic Axisymmetric Nozzle Boattail Drag Computer Program and a potential flow method developed by Lt. Thomas J. Plant of AFFDL/FXM (Reference 3), were
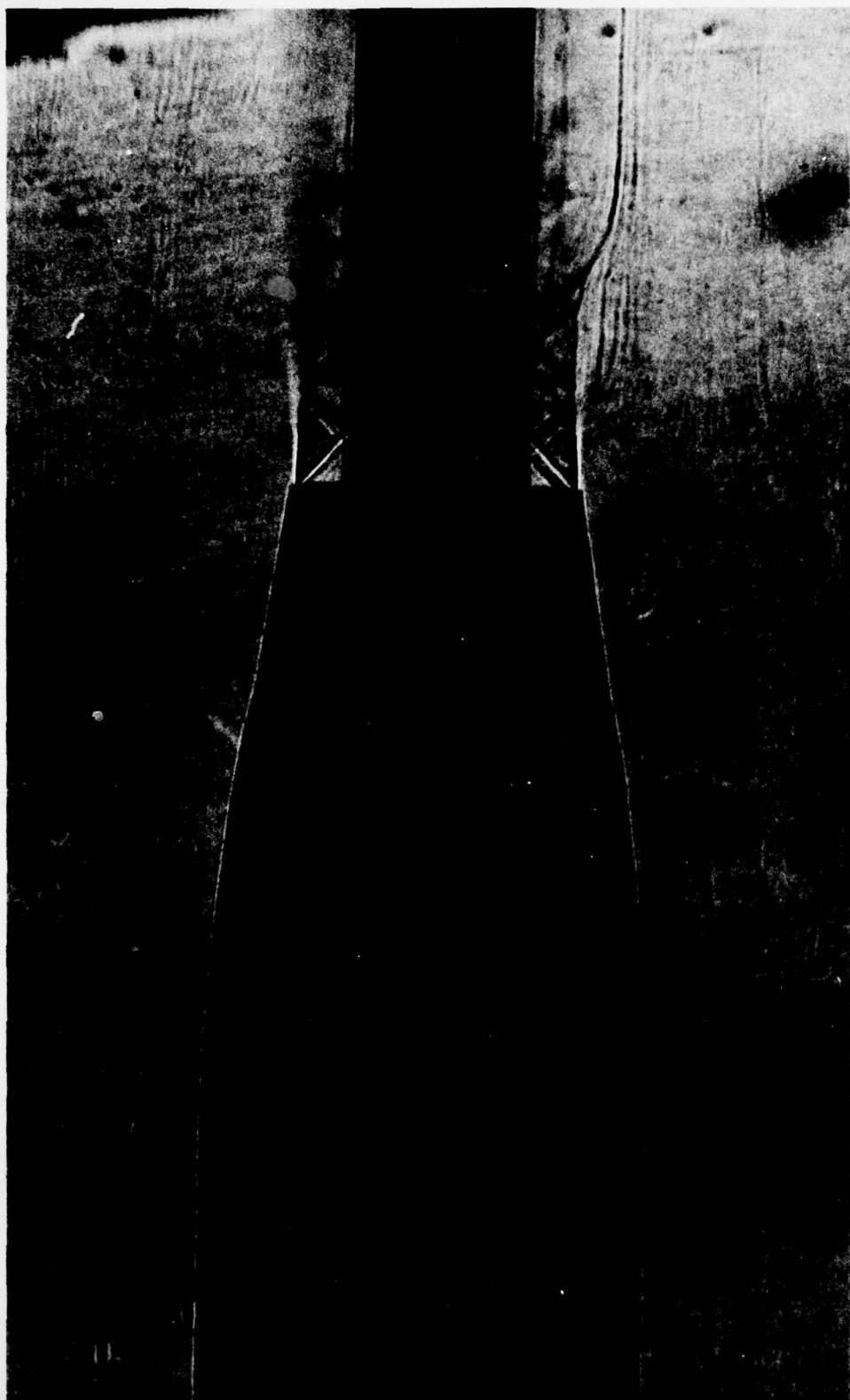
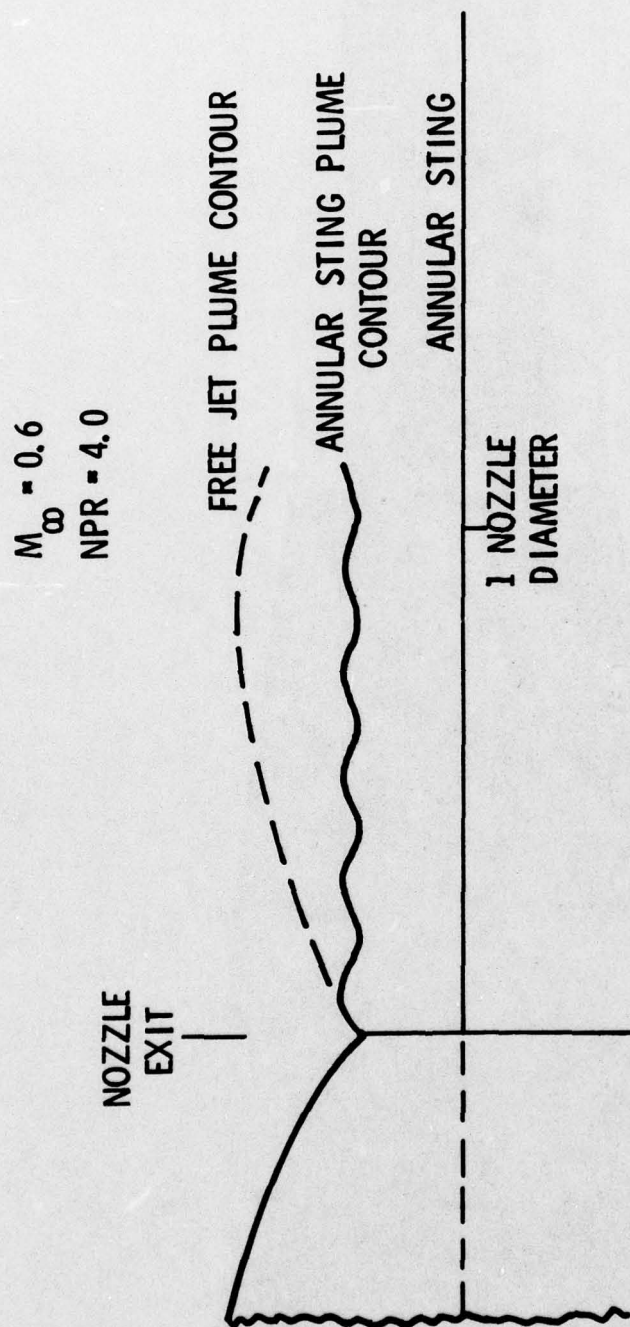Figure 21. Reheat Nozzle; Annular Sting Plume Contour Schlieren, $M_\infty = 0.6$

$M_\infty = 0.6$
$NPR = 4.0$

FREE JET PLUME CONTOUR

ANNULAR STING PLUME CONTOUR

ANNULAR STING

NOZZLE EXIT

1 NOZZLE DIAMETER

Figure 22. Cruise Nozzle; Free Jet and Annular Sting Plume Contours

46

$M_\infty = 0.8$
$NPR = 4.0$

FREE JET PLUME CONTOUR
ANNULAR STING PLUME CONTOUR
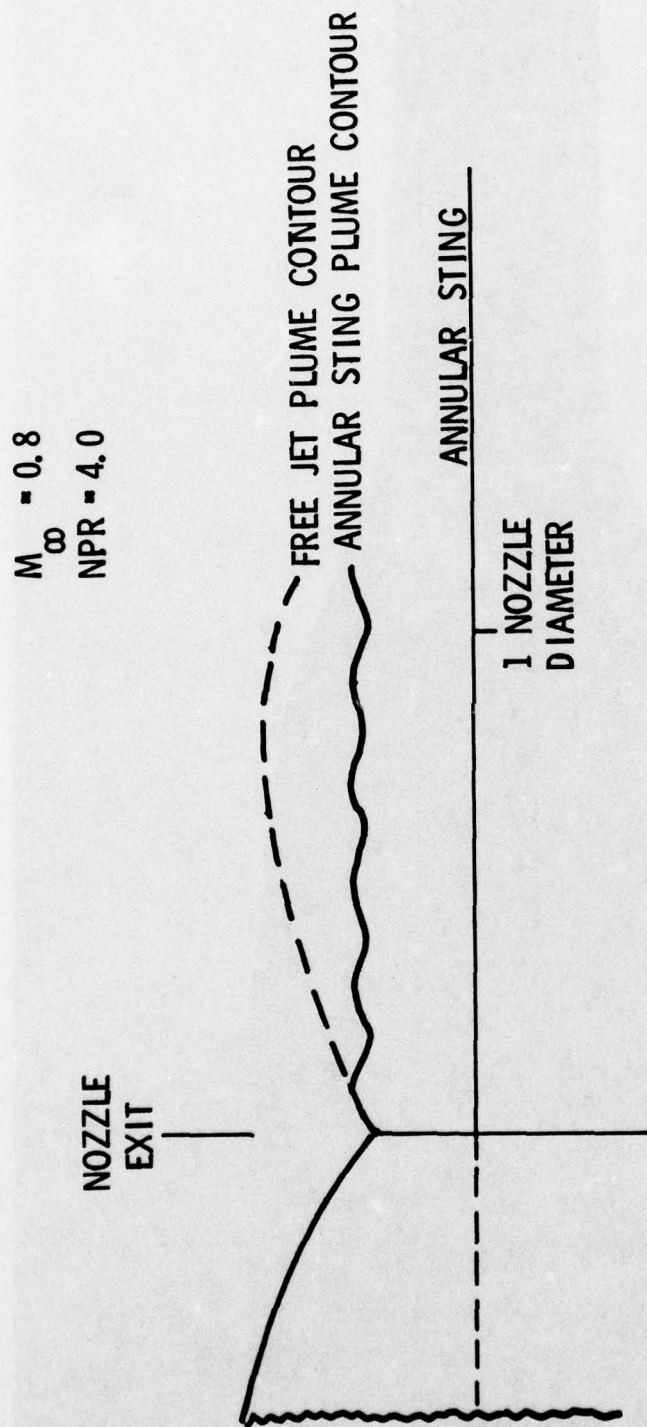
ANNULAR STING

1 NOZZLE
DIAMETER

NOZZLE
EXIT

Figure 22. (Concluded)

Figure 23. Cruise Nozzle; Annular Sting Plume Contour Schlieren, $M_\infty = 0.6$

input with annular sting geometric characteristics and executed on the Aeronautical Systems Division (ASD) computer system at Wright-Patterson AFB, Ohio. The latter method was also used to obtain the approximate values for the solid wind tunnel wall effects on the aftbody/boattail pressure distributions.

The Subsonic Axisymmetric Nozzle Boattail Drag Computer Program is an incompressible potential flow method coupled with a Gothert transformation to account for compressibility. This computer code has a provision for a turbulent boundary layer calculation which becomes a modified displacement thickness for the axisymmetric body potential flow solution. The exhaust plume is calculated by a combined shock-expansion/one-dimensional method. The internal and external flow fields are iterated until the solution converges. The code is established for all subsonic flow only and is applicable to convergent, convergent-divergent, and plug nozzles with arbitrary external contours. This program was developed internally at the Lockheed California Company and upgraded and extended under an AFFDL/FXM contract.

The potential flow method developed by Lt. Plant is the solution of the exact velocity potential equations for arbitrary axisymmetric bodies. The flow field is mapped by a natural coordinate system with a variable upper boundary. The wind tunnel wall effects are approximated by a solid wall at the wind tunnel wall station. The exhaust plume is assumed to be a cylinder and the flow field is limited to subcritical flow. This method compares well with axisymmetric body experimental data.

Comparisons of the analytically predicted aftbody boattail pressure distributions with the actual wind tunnel data is shown in Figures 24 and 25. To compare on an even basis, inviscid pressure distributions for both analytical methods are shown with free air boundaries and cylindrical exhaust plumes. The pretest predictions did very well in locating the maximum expansion point in the pressure distribution and in indicating the general trend of the recompression. Both methods diverge from the wind tunnel data near the nozzle exit at the discontinuity formed by the nozzle exit and exhaust plume. In general, the methods predict the
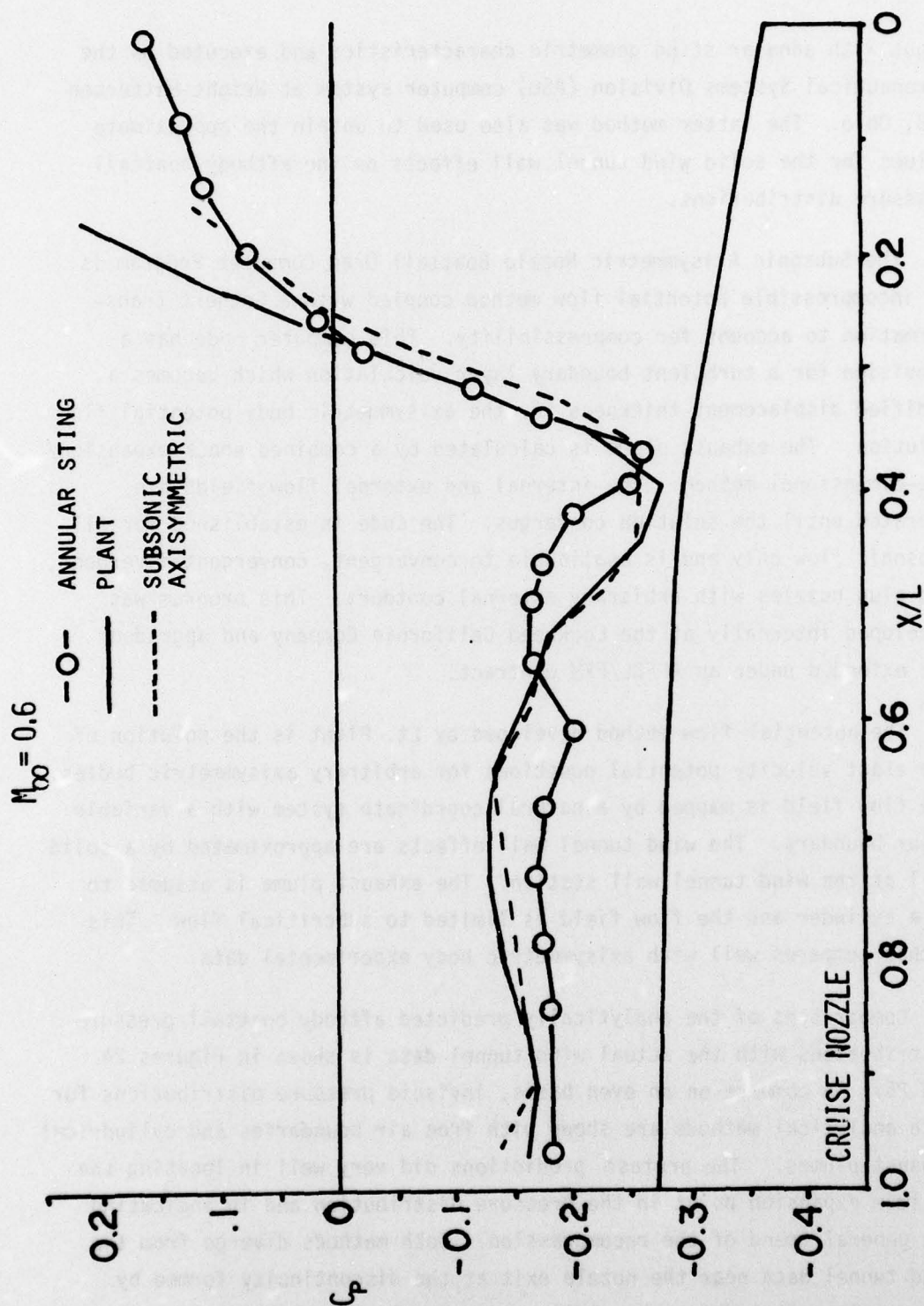
49

Figure 24. Cruise Nozzle; Comparison of Analytical Pressure Coefficient Distributions with Annular Sting Wind Tunnel Data

$M_\infty = 0.8$

○ ANNULAR STING
—— PLANT
---- SUBSONIC
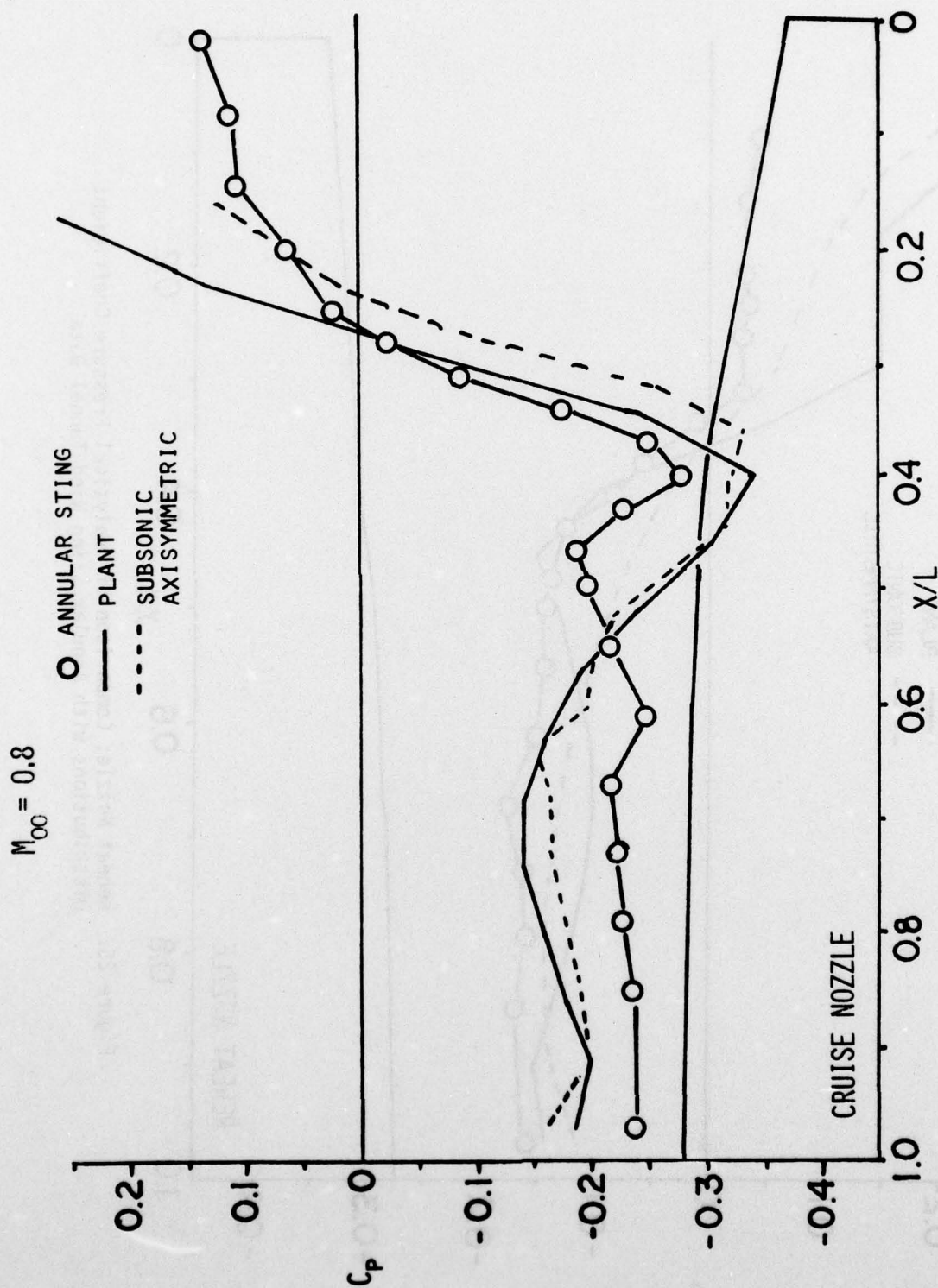AXISYMMETRIC

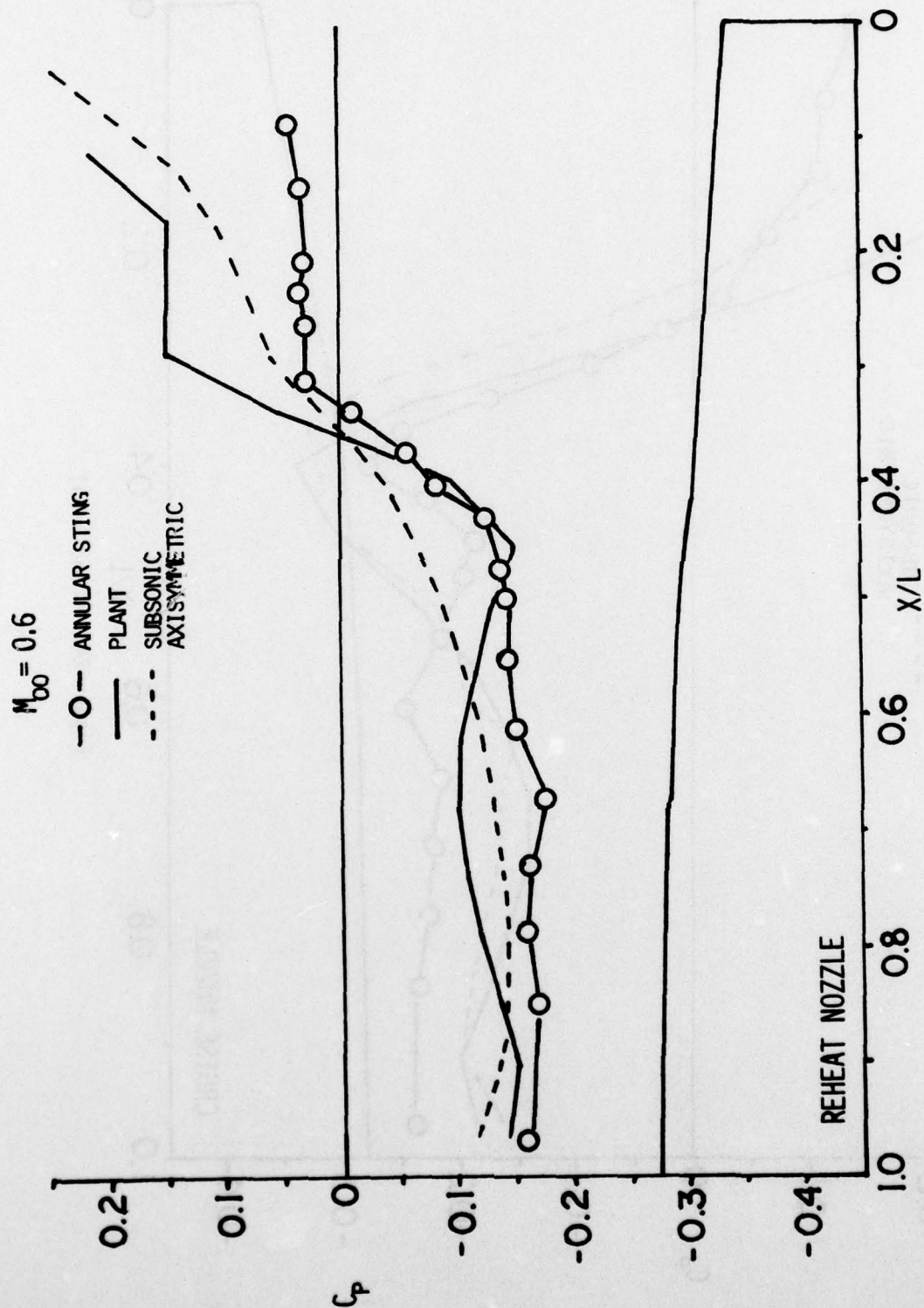CRUISE NOZZLE

Figure 24. (Concluded)

51

Figure 25. Reheat Nozzle; Comparison of Analytical Pressure Coefficient Distributions with Annular Sting Wind Tunnel Data
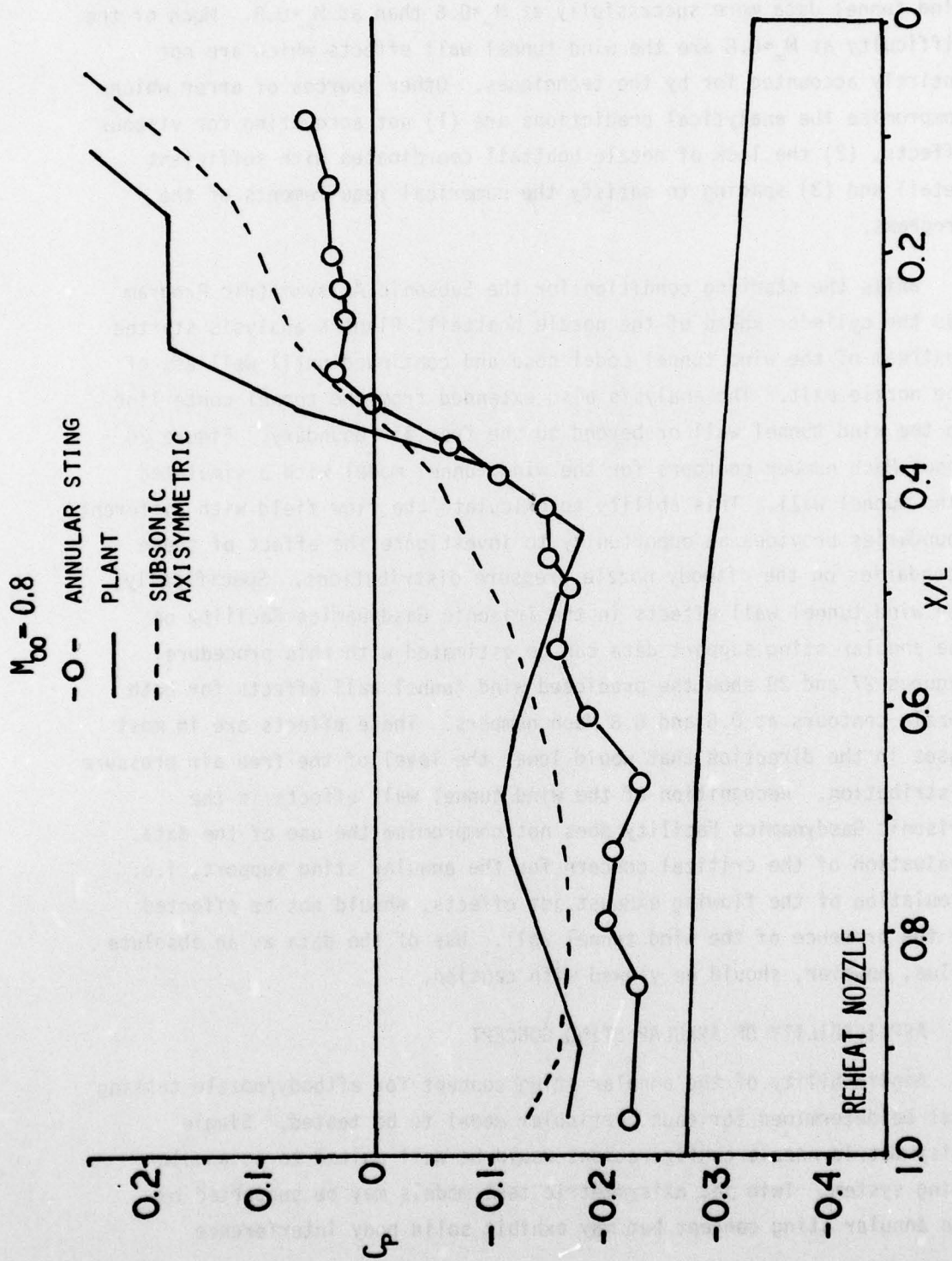
Figure 25. (Concluded)

wind tunnel data more successfully at $M_\infty=0.6$ than at $M_\infty=0.8$. Much of the difficulty at $M_\infty=0.8$ are the wind tunnel wall effects which are not entirely accounted for by the techniques. Other sources of error which compromise the analytical predictions are (1) not accounting for viscous effects, (2) the lack of nozzle boattail coordinates with sufficient detail and (3) spacing to satisfy the numerical requirements of the programs.

While the starting condition for the Subsonic Axisymmetric Program was the cylinder ahead of the nozzle boattail, Plant's analysis started upstream of the wind tunnel model nose and continued until well aft of the nozzle exit. The analysis also extended from the tunnel centerline to the wind tunnel wall or beyond to the free air boundary. Figure 26 shows Mach number contours for the wind tunnel model with a simulated wind tunnel wall. This ability to calculate the flow field with different boundaries provides an opportunity to investigate the effect of these boundaries on the aftbody nozzle pressure distributions. Specifically, the wind tunnel wall effects in the Trisonic Gasdynamics Facility on the annular sting support data can be estimated with this procedure. Figures 27 and 28 show the predicted wind tunnel wall effects for both nozzle contours at 0.6 and 0.8 Mach numbers. These effects are in most cases in the direction that would lower the level of the free air pressure distribution. Recognition of the wind tunnel wall effects in the Trisonic Gasdynamics Facility does not compromise the use of the data. Evaluation of the critical concern for the annular sting support, i.e. simulation of the flowing exhaust jet effects, should not be affected by the presence of the wind tunnel wall. Use of the data as an absolute value, however, should be viewed with caution.

7. APPLICABILITY OF ANNULAR STING CONCEPT

Applicability of the annular sting concept for aftbody/nozzle testing must be determined for each particular model to be tested. Single axisymmetric nozzle configurations would be well suited to an annular sting system. Twin jet axisymmetric test models may be supported by the annular sting concept but may exhibit solid body interference
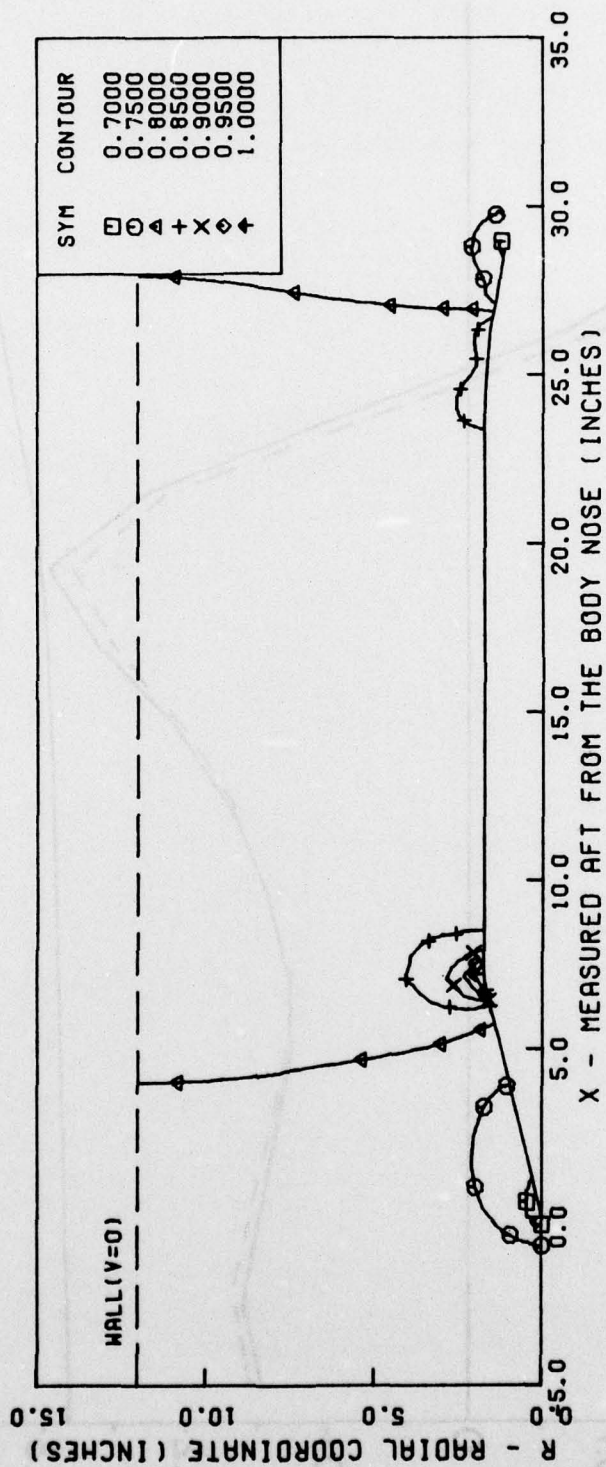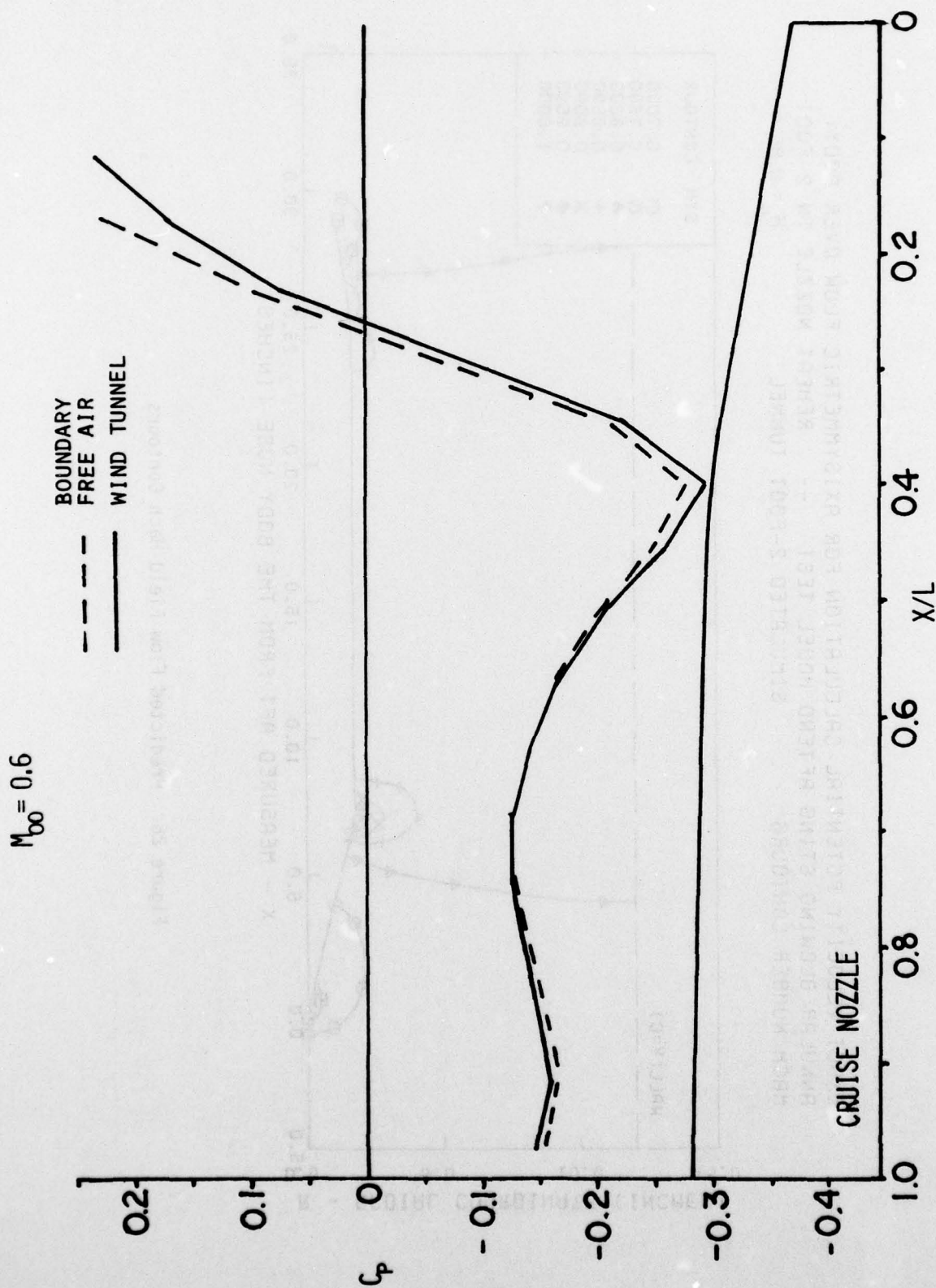
Figure 26. Predicted Flow Field Mach Contours

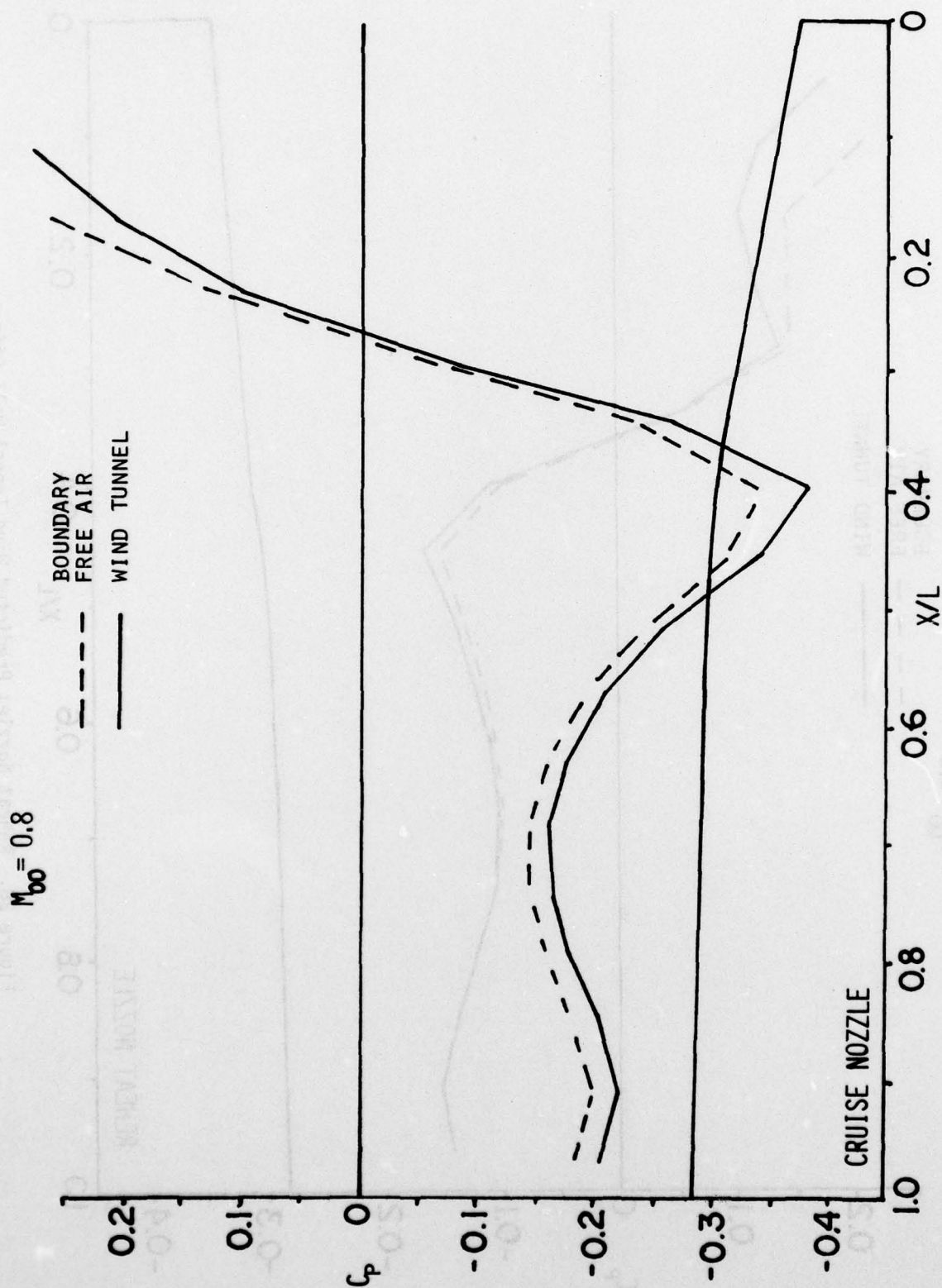Figure 27. Cruise Nozzle; Predicted Wind Tunnel Wall Effects
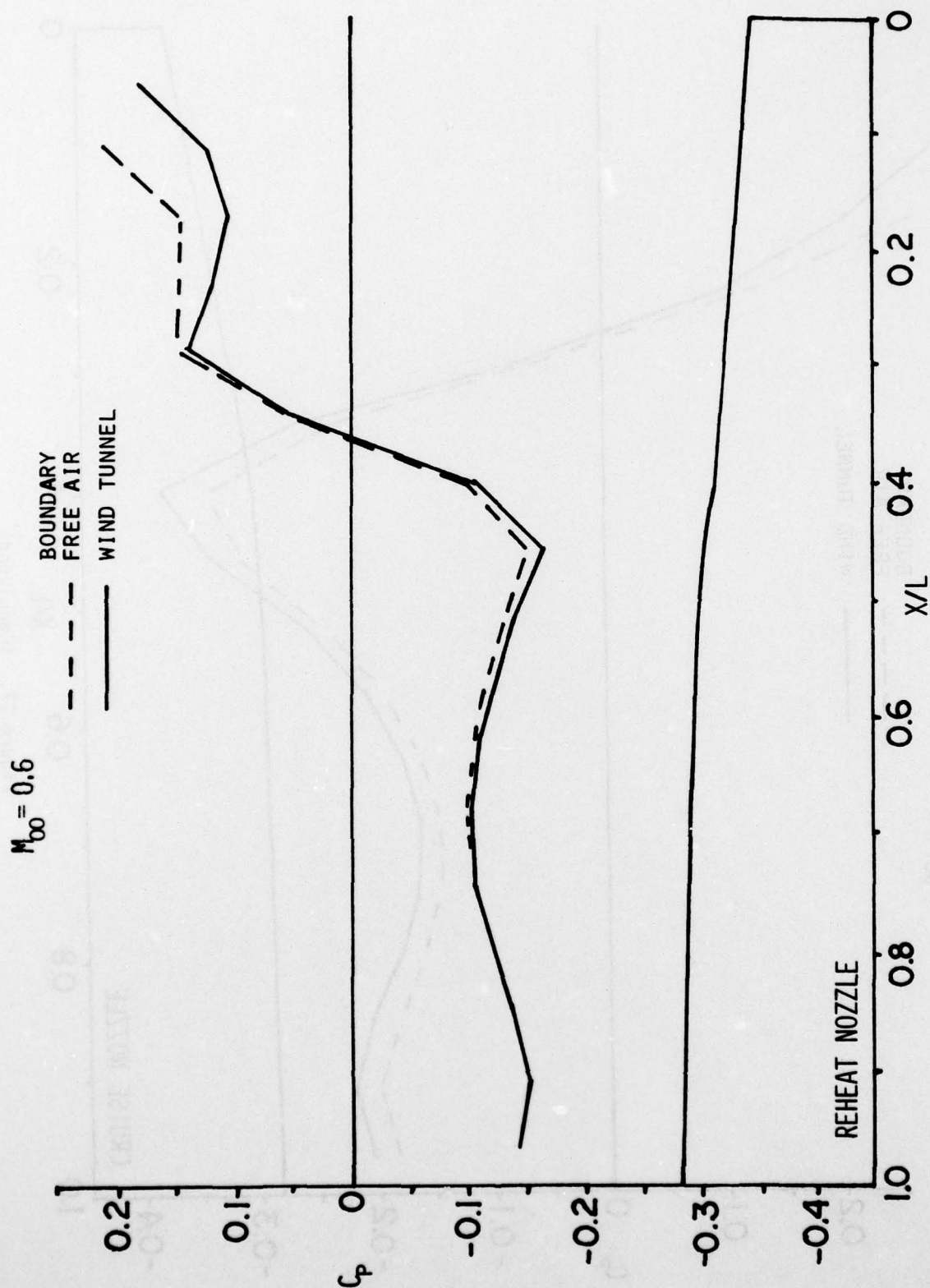
Figure 27. (Concluded)

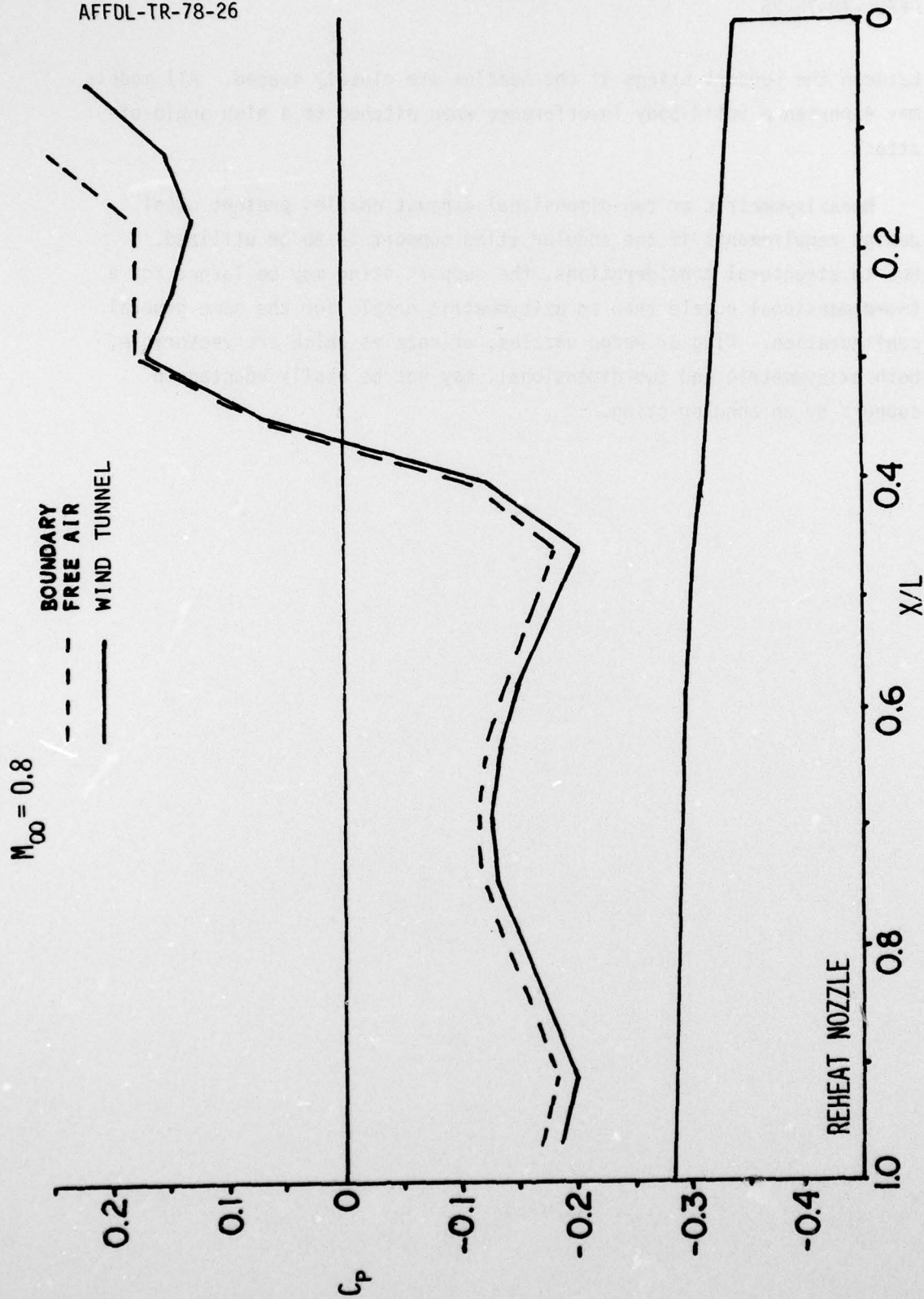Figure 28. Reheat Nozzle; Predicted Wind Tunnel Wall Effects

Figure 28. (Concluded)

between the support stings if the nozzles are closely spaced. All models may experience solid body interference when pitched to a high angle-of-attack.

Nonaxisymmetric or two-dimensional exhaust nozzles present usual design requirements if the annular sting support is to be utilized. Due to structural considerations, the support sting may be larger for a two-dimensional nozzle than an axisymmetric nozzle for the same general configuration. Plug or wedge nozzles, or nozzles which are vectorable, both axisymmetric and two-dimensional, may not be easily adapted to support by an annular sting.
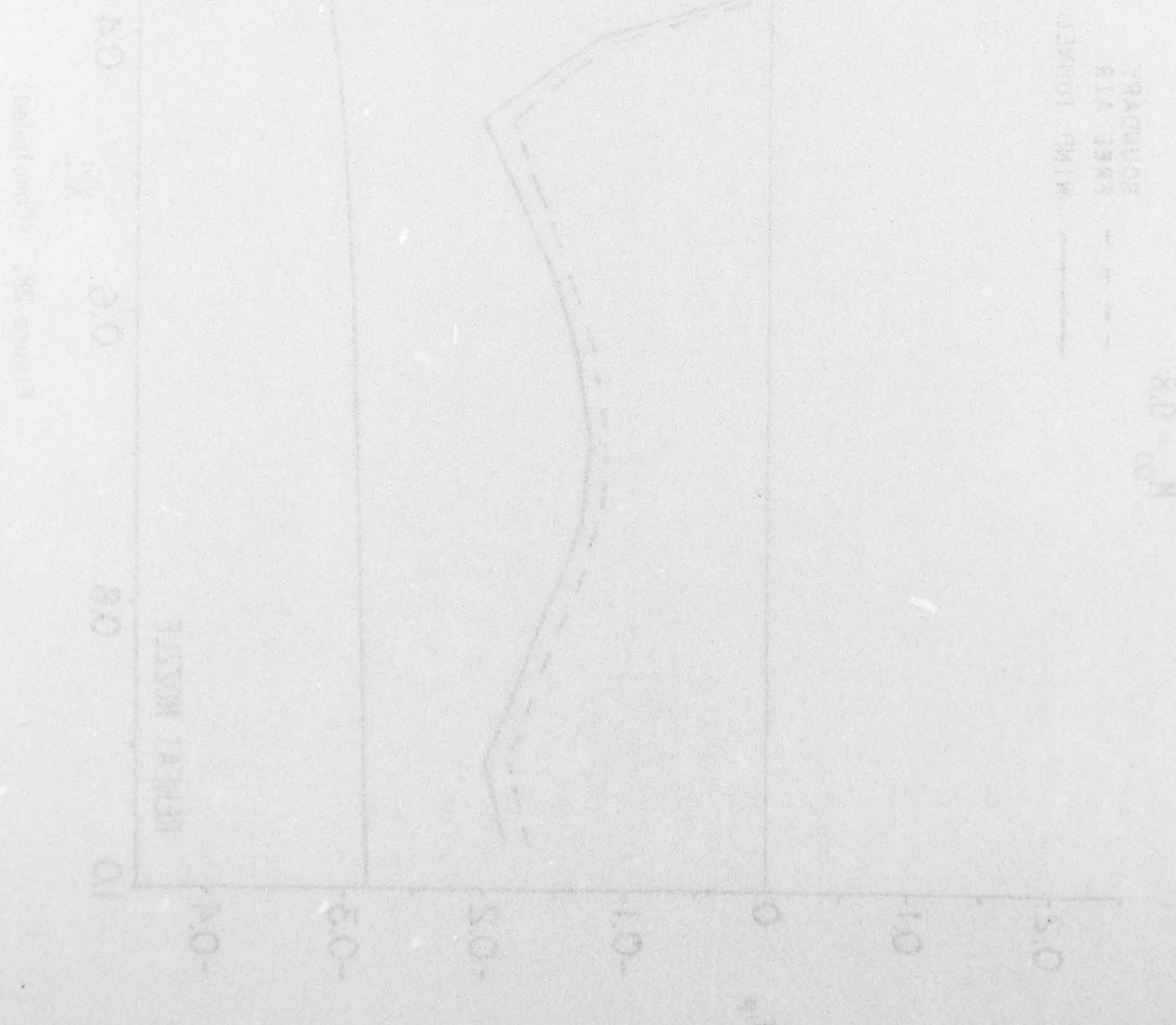
SECTION III

CONCLUSIONS AND RECOMMENDATIONS

Based on the evaluation of the test apparatus and the test results the following conclusions and recommendations can be drawn:

1. A mechanically feasible test apparatus for the annular sting system has been designed, fabricated, and successfully tested.

2. Care must be taken when internal nozzle parameters are being designed into the test nozzles to ensure equivalent free jet internal nozzle flow.

3. Facility and model differences are evident in the initial portion of the nozzle boattail pressure distributions. These differences are not believed to effect the evaluation of the annular sting jet effects.

4. The annular sting reheat nozzle shows good jet effects when compared to the free jet nozzle jet effects. Above moderate nozzle pressure ratios, however, the reheat nozzle appears to be limited in mass flow to provide adequate jet effects.

5. The annular sting cruise nozzle exhibits a solid body influence of the support sting and fails to properly simulate the jet effects of a full flowing exhaust nozzle.

6. Further evaluation must be conducted to determine an optimum relationship of the nozzle throat flow area, support sting diameter, and nozzle mass flow for the requirements of model support and simulation of nozzle jet effects.

7. The presence of the solid support sting affects the basic plume structure of the annular sting nozzle.

8. Both the Subsonic Axisymmetric Nozzle Boattail Drag Computer Program and Lt. Plant's exact potential flow analysis predicted the nozzle boattail pressure distributions reasonably well.

9. Applicability of the annular sting concept for aftbody nozzle testing must be determined for each particular proposed test model.

AFFDL-TR-78-26

REFERENCES

1. Bittrick, W. C., _Light Weight Fighter Nozzle Model Test with Faired Aft-Fuselage_, General Dynamics Report MR-P-348, General Dynamics Corp., Fort Worth, Texas, February 1973.

2. White, H. L., _Trisonic Gasdynamic Facility User Manual_, AFFDL-TM-73-82 FXM, Air Force Flight Dynamics Laboratory, Wright-Patterson AFB, Ohio, June 1973.

3. Plant, Lt. Thomas J., _An Exact Potential Solution of Steady Compressible Flow Over Arbitrary Two-Dimensional and Axisymmetric Bodies in Simply Connected Fields_, AFFDL-TR-77-116, Air Force Flight Dynamics Laboratory, Wright-Patterson AFB, Ohio, October 1977.